2019-01-01

Quasi-Harmonic And Anharmonic Entropies In Transition Metals

Bimal K C
University of Texas at El Paso

QUASI-HARMONIC AND ANHARMONIC ENTROPIES IN TRANSITION METALS

BIMAL K C

Master's Program in Physics

APPROVED:

Ramon Ravelo, Ph.D., Chair

Rajendra Zope, Ph.D.

Russel Chianelli, Ph.D.

Stephen L. Crites, Jr., Ph.D.
Dean of the Graduate School

To my

parents who are supporting me from 8239 miles away

♡

QUASI-HARMONIC AND ANHARMONIC ENTROPIES IN TRANSITION METALS

by

BIMAL K C, MS

THESIS

Presented to the Faculty of the Graduate School of

The University of Texas at El Paso

in Partial Fulfillment

of the Requirements

for the Degree of

MASTER OF SCIENCE

Department of Physics

THE UNIVERSITY OF TEXAS AT EL PASO

December 2019

Acknowledgements

This thesis work would have been much harder if there was no support of few but important persons. First of all, I would like to express my sincere gratitude to my supervisor Dr. Ramon Ravelo for his patience, motivation and immense knowledge. His academic parenting helped me all the time during my research and thesis work.

I would also like to thank members of my thesis committee, Dr. Rajendra Zope of the Physics Department and Dr. Russell Chianelli, of the Department of Chemistry and Biochemistry, all at the University of Texas at El Paso.

I wish to thanks Madawa Abeywardhana and Celia Garcia for the insightful comments, encouragement, discussion and the joyful moment we have spent together.

I am very grateful to my lovely wife, Samikshya K C and my lovely daughter, Aarunya K C whose support is indispensable through the years.

Abstract

Density functional theory (DFT) employing the quasi-harmonic approximation (QHA) is a robust method for evaluating thermal properties of solids. In the case of transition metals however, the method yields high values of the thermal pressure when compared to experimental data or with more direct methods like quantum-molecular dynamics (QMD) simulations. Surprisingly, there has not been to date, a systematic study aimed at understanding the reasons for these large discrepancies, particularly at low temperature, i.e. below the Debye temperature of the solid. Using Tantalum as a test model for which a lot of experimental data exist, thermal properties were evaluated employing direct molecular dynamics (MD) simulations and compared to QHA predictions. The atomic interactions were modeled using an embedded-atom method (EAM) potential for Ta fit to a large data set of ab-initio data. The free energy and entropies are computed as a function of temperature with MD employing the adiabatic switching formalism at zero and 50 GPa. Compared with the quasi-harmonic entropy computed within QHA, the anharmonic entropy is large even at moderately low temperatures, suggesting that phonon frequencies are temperature-dependent at low temperatures but this dependence is significantly less important at high temperatures, where volume-dependence dominates.

Table of Contents

List of Tables

List of Figures

Chapter 1: Introduction

If we heat the solid at zero pressure, the atoms in solid starts to vibrate and vibration of the atomic lattice are responsible for all thermal properties which is associated with material response to temperature. Thermal properties at high temperature, is directly related to thermal expansion and to the thermal pressure. At fixed volume, then internal energy of solid changes and thus we can describe the temperature dependence of thermal pressure via proportionality constant termed Gruneisen parameter. The thermal expansion coefficient of the solid at different pressure is directly related to the Grüneisen parameter of the solid at the appropriate pressure. Experimentally, it is very difficult to obtained the expansion coefficient at high pressure and equation of state (EOS) of materials at high pressures rely heavily on models and/or computational evaluations of the Grüneisen parameter.

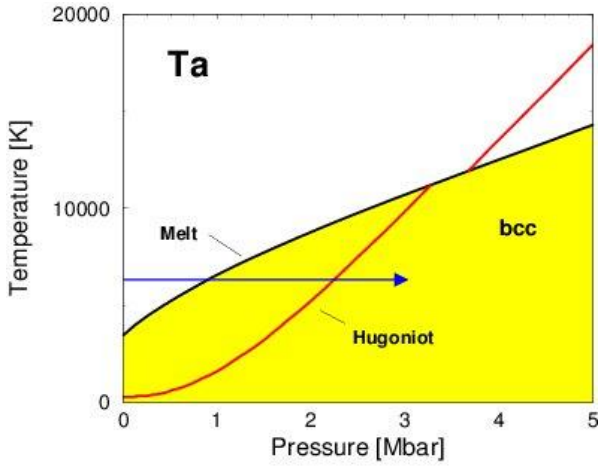

Figure 1.1: Phase diagram of tantalum. Black curve is the melt line and red line is the principle Hugoniot (EOS) and arrow shows the isothermal compression.

The pressure can be written as:

$$P(V,T) = P(V,0) + \frac{\gamma C_V T}{V}$$

where, P_{tot} (V, T) is the total pressure, P (V, 0) is the pressure at given volume V at T=0K, γ is the Grüneisen parameter and C_V is the specific heat at constant volume.

The EOS is very important to study the thermal properties of solid. Models that properly reproduce the thermal pressure are very important to accurately predict EOS and describes how temperature and pressure effects the behavior of solids. Thus, to properly reproduced accurate EOS curves, one focus is the proper evaluation of Grüneisen parameter.

First principle calculations are commonly used to evaluate the Grüneisen parameter employing the quasi-harmonic approximation method. The method however, (DFT-QHA) in the case of transition metals, shows strong disagreement with more direct methods like quantum molecular dynamics (QMD) calculations.

Grüneisen [1] assumed that the modal Gruneisen $\gamma = -\frac{\partial \ln w}{\partial \ln V}$ is same for all frequencies of the solid and independent of temperature. Cohen and Gulseren [2] studied the thermal equation of state of Tantalum (Ta) employing first principles using full potential linearized augmented plane wave (LAPW) within QHA and concluded that electronic excitations contribute to variations in the Grüneisen parameter. Taioli et.al. [3] studied via DFT the pressure and temperature dependence of the Grüneisen parameter in Ta neglecting the electronic contribution to the free energy of the solid.

Surprisingly, the disagreement between the methods is largest at low temperatures (between room temperature and the Debye temperature, which for Ta is T_D=246 K) when the volumetric anharmonicity should be less and the system should be more harmonic. The first three Brillouin zones Grüneisen parameter as a function of temperature from first principles calculations employing the quasi-harmonic approximation [2, 3], quantum MD simulations [4] and the experimental [5] value at zero pressure and room temperature.

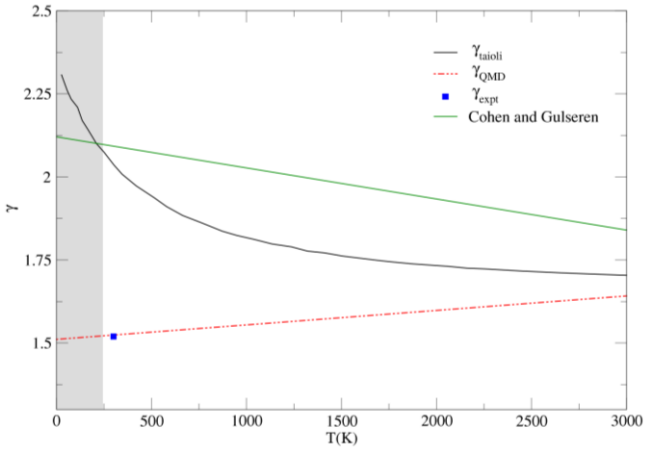

Figure 1.2: The comparison between the first principle calculations of Taioli et al [3], Cohen and Gulseren [2], the results from quantum molecular dynamics simulations (Ravelo and Holian [4]) and the experimental value at zero pressure and room temperature.

The quasi-harmonic approximation (QHA) is one of the most frequently used method to calculate thermal properties within DFT. However, QHA does not seem to work well for transition metals (Mo, Ta, W) and there is no systematic method to predict the accuracy of an EOS obtained using QHA to account for the thermal pressure. One limitation can be due to the fact that QHA does not take the account of temperature dependence of phonon frequencies. In my thesis I study via direct comparisons the thermal properties obtained via molecular dynamics simulations with those obtained using the QHA method. In the next chapters I review the QHA formalism followed by MD techniques employed in my research.

Anharmonic contributions to the free energy and entropy can come indirectly from the temperature via volume changes through the expansion coefficient and directly from an explicit temperature-dependence of the phonon frequencies. By directly computing the ionic entropy within molecular dynamic the anharmonic contribution can be computed from its difference with the quasi-harmonic entropy which includes only a volume correction but no direct temperature

effects. This study will definitely advance our understating of anharmonic contributions to thermal pressure and expansion coefficient of transition metals.

Transition metals are d-block elements with high density, high melting points and boiling points. Tantalum is a bcc transition metal with high melting temperature and strength. Hence it is widely used to produce high-temperature super alloys that can be used for various technological applications. It has a simple phase diagram with highly stable bcc phase with no known phase transformations, which allows it to be used for high pressure calibration of shock data.

My thesis outline is as follows:

- In **chapter 2**, the introduction to lattice dynamics, Brilloiun zone and phonons are presented.
- **Chapter 3** describes about introduction and thermodynamics of the quasi-harmonic approximation (QHA) method. The thermal properties of phonons are also summarized in this chapter.
- **Chapter 4** deals with Molecular Dynamics (MD) methods that are required to carry out the atomistic simulations under different ensembles in consideration. This chapter also explains the formalism of Embedded Atom Method (EAM) which is carried out to model atomic interaction and statistical ensembles.
- C**hapter 5** includes the method that we used to calculate the properties of tantalum. Also, the results of our present work are shown where we have compared our MD data with QHA data.
- Finally, summary and conclusions are presented in **chapter 6**.

Chapter 2: Lattice Dynamics

The lattice dynamics deals with the study of the atomic vibrations in a crystal. in crystals, the propagation of sound waves is the example of the role of lattice dynamics. Lattice dynamics also gives us properties such as thermodynamics, phase transition, thermal expansion, superconductivity, thermal conductivity, etc.

In lattice dynamics, the atomic motion is described as harmonic travelling waves and can be fully characterized in terms of its wavelength (λ), angular frequency (ω), amplitude and direction in which they travel. But rather than using _ we can use wave vector k which is a vector defined in the direction parallel to propagation of wave and normalized such that $|\mathbf{k}| = \frac{2\pi}{\lambda}$. It is seen that there are conservation laws which are much easier to handle in terms of k rather than λ.

2.1 Lattice Structure

In Bravais lattice, the unit cell of bcc is defined by the three lattice vectors given as

$$\boldsymbol{a_1} = \frac{a}{2}\begin{pmatrix} 1 \\ 1 \\ -1 \end{pmatrix} \quad , \boldsymbol{a_2} = \frac{a}{2} \quad \begin{pmatrix} 1 \\ -1 \\ 1 \end{pmatrix} \quad , \boldsymbol{a_3} = \frac{a}{2} \quad \begin{pmatrix} -1 \\ 1 \\ 1 \end{pmatrix} \tag{2.1}$$

The reciprocal lattice exists in reciprocal (k- or momentum) space and is the Fourier transformation of direct (Bravais) lattice. The reciprocal lattice plays a vital role in studies of periodic structures and the diffraction pattern of a crystal. The atomic arrangement of a crystal can be inferred by this process. The reciprocal lattice vectors are constructed with identity, such that with $\mathbf{b}_i . \mathbf{a}_j = 2\pi\delta_{ij}$.

$$\boldsymbol{b_1} = \frac{\pi}{a}\begin{pmatrix} 1 \\ 1 \\ 0 \end{pmatrix} \quad , \boldsymbol{b_2} = \frac{\pi}{a} \quad \begin{pmatrix} 1 \\ 0 \\ 1 \end{pmatrix} \quad , \boldsymbol{b_3} = \frac{\pi}{a} \quad \begin{pmatrix} 0 \\ 1 \\ 1 \end{pmatrix} \tag{2.2}$$

and $\mathbf{a}_j$ is j^{th} primitive (direct) lattice vector and δ_{ij} is Kronecker delta function.

2.2 BRILLOUIN ZONE

Brilloiun zone was first introduced by a French physicist Leon Brilloiun in 1930 [6]. A Brillouin zone is a choice of the unit cell of the reciprocal lattice. The first Brillouin zone is defined as the smallest volume entirely enclosed by the planes formed by perpendicular bisectors of the reciprocal lattice vectors which are drawn from origin.

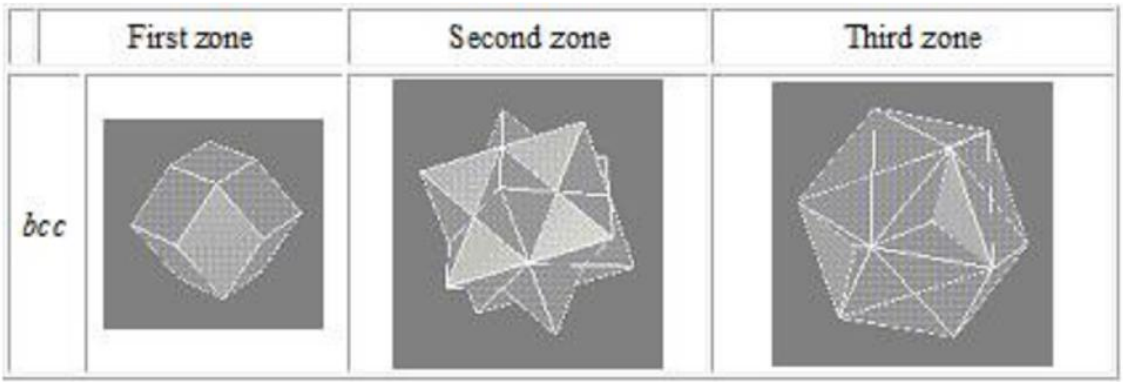

Figure 2.1: The first three Brillouin zones for bcc lattice illustrated.

In other words, the first Brillouin zone is a geometrical construction to the Winger-Seitz primitive cell in the k-space. Brilloiun zone are very important to describe the electronic structure of solids. There are also first, second, third, etc., Brillouin zone with same volume the regions located at increasing distance from origin. Irreducible Brillouin zone (IBZ) is the smallest wedge of first Brillouin zone (figure 2.3) such that wave vector k of IBZ can be used to obtain any wave vector k in first Brillouin zone by performing symmetry operation in any crystal structure.

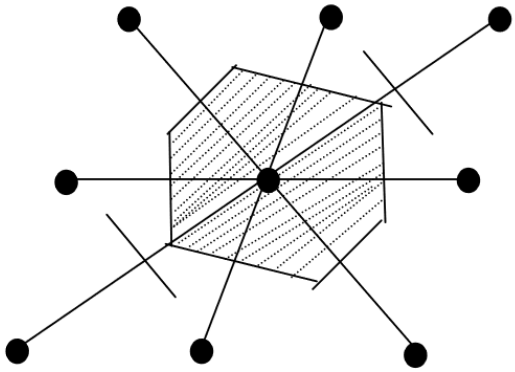

Figure 2.2: Construction of primitive Wigner-Seitz cell in 2-D direct space lattice

In bcc, the first irreducible wedge has four vertices (Γ, H, P and N) whose coordinates are shown in 2.3.

Choice of k points

k points are the sampling points in first Brillouin zone of the material, i.e. they represent the specific region of reciprocal-space which is very close to the Gamma point (origin). Monk horst and Pack [7] is the method of choosing a set of k points (these k points are the coordinates of a structure in momentum space) for the sampling the Brillouin zone according to which, the sampling **k** points are distributed uniformly in Brillouin zone with columns or rows of **k** points running parallel to reciprocal lattice vectors ($\mathbf{b}_1$, $\mathbf{b}_2$ and $\mathbf{b}_3$) which span Brillouin zone. The one corner of Brillouin zone is attached to the origin of coordinate system. The small polyhedra are The supplied k points pattern spread out over the whole Brillouin zone by the translations of tile.

$$\boldsymbol{k} = u * \boldsymbol{b_1} + v * \boldsymbol{b_2} + w * \boldsymbol{b_3} \tag{2.3}$$

where, u, v and w are supplied values.

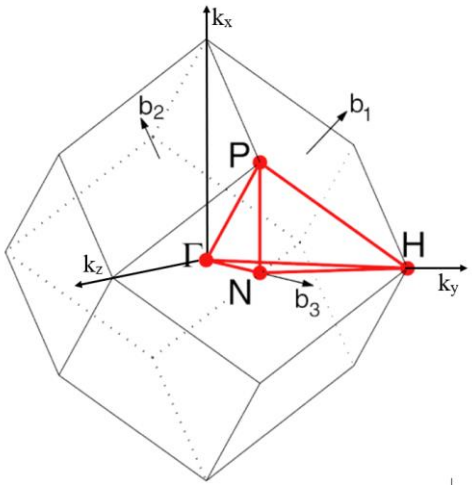

Figure 2.3: First Brilloiun zone of the BCC cell showing Γ, N, H and P as high symmetry points and axes, irreducible Brillouin zone (in red). Coordinates the symmetry points coordinates (u, v, w) in the primitive basis $\mathbf{b}_1$, $\mathbf{b}_2$, $\mathbf{b}_3$ and Cartesian coordinates k are shown in the table on the right. $\mathbf{k}_x$, $\mathbf{k}_y$, $\mathbf{k}_z$ are the primitive reciprocal basis vectors.

2.3 PHONONS

Generally, the lattice structure (crystal) is rigid at T=0K but at finite temperature, due to the thermal effect, the atoms in crystal vibrate around equilibrium [8]. The interaction between particles in a crystal can be described by a potential which is used to derive the equations of motion of the atoms. The solution of the equations of motions can be obtained with the help of Bloch's Theorem. The solutions thus obtained are collective waves and obey the periodicity of the lattice and the relation between the frequency and the reciprocal lattice vectors is given by the dispersion relation w(**k**).

However, being part of periodic lattice, the atoms cannot move freely and the motion of single atom is affected by the movements of the other atoms in a lattice. So, all the atoms vibrate collectively according to a periodic wave solution that perfectly matches the periodicity of the lattice, called phonons.

Generally, Phonons are divided into two branches: the acoustic branch and the optical branch [9]. The acoustic branch corresponds to the propagation of sound waves in which direction of propagation of atoms are in same direction and tends to zero for small wave vectors k. In optical branch, atoms show out of phase movement and has higher frequencies for **k** = 0. If we consider lattice with only one atom basis, then only the acoustic branch appears, whereas for a lattice with a two-atom basis, the optical becomes visible.

Phonon Dispersion

To estimate phonon dispersion relation, we first use the harmonic approximation which assumes that atoms in crystal oscillate around equilibrium with a deviation such that they are small compared to interatomic distance. Thus, potential V as a function of atomic displacement (u_α(**l**k)) is given as

$$\mathrm{V} = V_0 + \sum_{\mathrm{lk}\alpha} \frac{\partial V}{\partial u_\alpha(\mathbf{l}\mathrm{k})} u_\alpha(\mathbf{l}\mathrm{k}) + \frac{1}{2} \sum_{\mathrm{lk}\alpha,\boldsymbol{l}'\mathrm{k}'\alpha'} \frac{\partial^2 V}{\partial u_\alpha(\mathbf{l}\mathrm{k}) \partial u_\beta(\mathbf{l}'\mathrm{k}')} u_\alpha(\mathbf{l}\mathrm{k})\, u_\beta(\mathbf{l}'\mathrm{k}') \qquad (2.4)$$

where, each unit cell has n atoms with labelled k and thus position is given by $\mathbf{r}_\mathrm{k}$ with respect to origin. The first term is constant and second term is zero at equilibrium, thus only term with second derivative in above equation is important which is also called force constant. *i.e.;*

$$\phi_{\alpha\beta}\left(\mathbf{l}k, \mathbf{l}'k'\right) = \frac{\partial^2 V}{\partial u_\alpha(\mathbf{l}\mathrm{k}) \partial u_\beta(\mathbf{l}'\mathrm{k}')} \qquad (2.5)$$

The force constant matrix explains the force on atom (**l**k) due to displacement of other atoms.

$$F_\alpha(\mathbf{l}k) = \frac{\partial V}{\partial u_\alpha(\mathbf{l}k)} \approx \sum_{\mathrm{l}'\mathrm{k}'\beta} \frac{\partial^2 V}{\partial u_\alpha(\mathbf{l}k) \partial u_\beta(\mathbf{l}'k')} u_\beta(\mathbf{l}'k')$$

$$= -\sum_{\mathrm{l'k'}\beta} \phi_{\alpha\beta}(\mathbf{l}k, \mathbf{l}'k')\, u_\beta(\mathbf{l}'k') \tag{2.6}$$

This force constant matrix is always symmetric

$$\frac{\partial^2 V}{\partial u_\alpha(\mathbf{l}k)\partial u_\beta\left(\mathbf{l}'k'\right)} = \frac{\partial^2 V}{\partial u_\beta(\mathbf{l}k)\partial u_\alpha\left(\mathbf{l}'k'\right)} \tag{2.7}$$

Even if we displace the lattice, the force on atom remains same which is also called the condition of translation of invariance.

$$\sum_{\mathrm{l'k'}} \phi_{\alpha\beta}\left(\mathbf{l}k, \mathbf{l}'k'\right) = 0 \tag{2.8}$$

Now, the equation of motion for each atom can be written as

$$m_k \ddot{u}(\boldsymbol{l}k) = \sum_{\mathrm{l'k'}\beta} \phi_{\alpha\beta}\left(\mathbf{l}k, \mathbf{l}'k'\right) u_{\alpha\beta}\left(\mathbf{l}'k'\right) \tag{2.9}$$

where, m_k is the mass of k_{th} atom and,

$$u_\alpha(\boldsymbol{l}k) = \frac{A_{\alpha,\mathrm{k(q)}}}{\sqrt{m_k}} e^{i(\boldsymbol{q}.R_i - w(\boldsymbol{q}).t)} \tag{2.10}$$

where, **q** is the wave vector corresponding to wave frequency w(**q**) at time t and A_α k(q) is amplitude of wave. Then using 2.5 and 2.6, we get,

$$\omega^2(\boldsymbol{q}) e^{i(\boldsymbol{q}.\boldsymbol{R}_i)} A_{\alpha\beta}(\mathbf{q}) = \sum_{\mathrm{l'k'}\beta} \frac{1}{\sqrt{m_k m_k'}} \phi_{\alpha\beta}\left(\mathbf{l}k, \mathbf{l}'k'\right) e^{i(\boldsymbol{q}.\boldsymbol{R}_i')} A_{\beta,k'}(\mathbf{q}) \tag{2.11}$$

rearranging above equation, we can write,

$$\omega^2(\boldsymbol{q}) A_{\alpha\beta}(\mathbf{q}) = \sum_{\beta k'} D_{\alpha\beta}(k, k', \boldsymbol{q}) A_{\beta,k'}(\mathbf{q}) \tag{2.12}$$

where, D_α(k; k'; **q**) is dynamical matrix and given by

$$D_{\alpha\beta}(k, k', \boldsymbol{q}) = \frac{1}{\sqrt{m_k m_k'}} \left[\sum_{\mathrm{l'k'}\beta} \frac{1}{\sqrt{m_k m_k'}} \phi_{\alpha\beta}\left(\mathbf{l}k, \mathbf{l}'k'\right) e^{i\boldsymbol{q}.(r_{i'} - \boldsymbol{R}_i)} \right] \tag{2.13}$$

Again,

$$[D_{\alpha\beta}(k,k',\boldsymbol{q})] *= D_{\alpha\beta}(k,k',\boldsymbol{q}) \tag{2.14}$$

which shows that the dynamical matrix is Hermitian. *i.e.*, it can be diagonalized and its eigen values are real. This can be solved if determinant of dynamical matrix is zero.

$$|D_{\alpha\beta}(k,k',\boldsymbol{q}) - \delta_{\alpha\beta}\delta_{kk'}\omega^2(\boldsymbol{q})| = 0 \tag{2.15}$$

where, square root of eigen value $\omega^2(\boldsymbol{q})$ gives phonon frequency and at every **q** there are 3n solutions (different branches) labelled by j. Generally, three phonon modes are present in mono atomic lattice. One is longitudinal mode where wave vector is parallel to atomic displacement vector and other two are called transverse modes where wave vector is normal to atomic displacement vector. Fig 2.3 represents the phonon dispersion that is obtained by diagonalization of dynamical matrix obtained from 2.11 and 2.12 for path connecting to the high symmetry point. Since, transverse branches are degenerate by symmetry so dispersion in path Γ-H-P-Γ has only two branches but for path Γ -N all three branches has different dispersion relation.

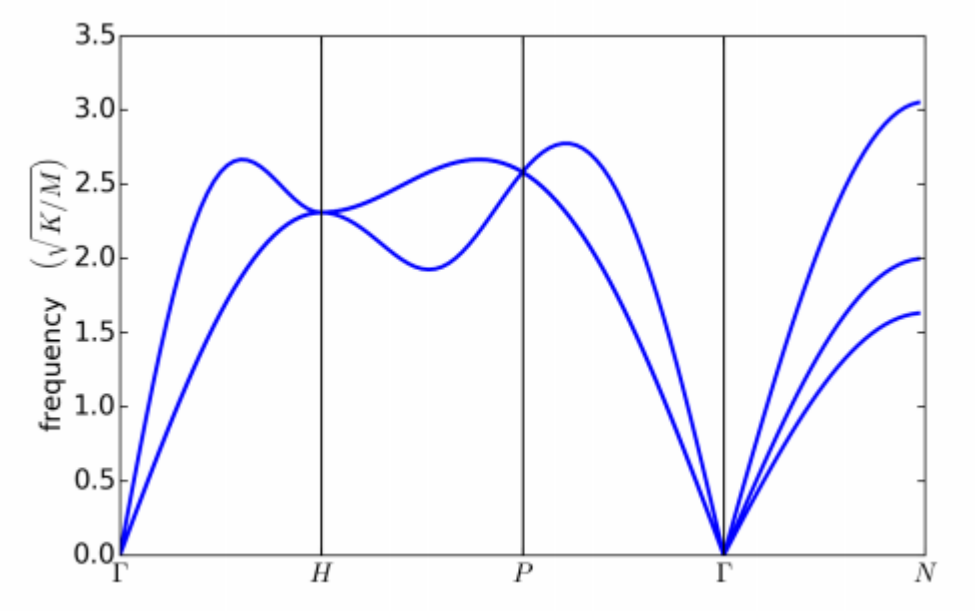

Figure 2.4: Phonon dispersion of a BCC crystal showing paths connecting to the high symmetry point Γ-H-P-Γ-N.

2.4 THERMAL PROPERTIES

In this section we study the connection between vibrational properties and thermodynamics of tantalum by recalling the relationship for thermodynamical properties derived from phonons frequencies.

2.4.1 Harmonic Oscillators

Classical Harmonic Oscillator

Let, w be the natural frequency of classical one-dimensional harmonic oscillator of mass M and force constant k such that

$$w = \sqrt{\frac{k}{M}} \tag{2.16}$$

and potential energy

$$V(x) = \frac{1}{2}kx^2 = \frac{1}{2}Mw^2x^2 \tag{2.17}$$

From equipartition theorem, the average kinetic ($\bar{E}$) and potential energies are equal. *i.e.*,

$$\bar{V}(x) = \bar{E} = \frac{1}{2}K_BT \tag{2.18}$$

Since, only x^2 depends on temperature and force constant k. So,

$$\overline{x^2} = \frac{K_BT}{Mw^2} = \frac{K_BT}{k} \tag{2.19}$$

Harmonic Phonons

If we consider a system of quantum harmonic oscillator with natural frequency w, then its occupation number at any temperature T is given by Bose-Einstein distribution. *i.e.*,

$$n(\hbar w, T) = \left(exp\left(\hbar w/_{K_BT}\right) - 1\right)^{-1} \tag{2.20}$$

And, the energy associated with it at thermal equilibrium ($w = w(\boldsymbol{qj})$) is given as:

$$E(\boldsymbol{qj}) = \left(n(\boldsymbol{qj}) + {}^{1}/_{2}\right) \hbar w(\boldsymbol{qj}) \tag{2.21}$$

where, $n(\boldsymbol{qj}) = n(\hbar w(\boldsymbol{qj}))$, then for Harmonic crystal,

$$E_H(\boldsymbol{qj}) = \sum_{\boldsymbol{qj}} E(\boldsymbol{qj}) = 3N \int_0^{w_{max}} \left(n(\boldsymbol{qj}) + {}^{1}/_{2}\right) \hbar w(\boldsymbol{qj}) g(w) dw \tag{2.22}$$

where, *g(w)dw* is phonon density of state (DOS).

The, entropy of any harmonic phonon of frequency *w* is given by

$$S_H(\boldsymbol{qj}, T) = K_B[(n+1)ln(n+1) - nlnn] \tag{2.23}$$

Thus, entropy per atom for harmonic system is

$$S_H(T) = \sum_{\boldsymbol{qj}} S_H(\boldsymbol{qj}, T) = 3K_B \int_0^{w_{max}} [(n+1)ln(n+1) - nlnn]\, g(w) dw \tag{2.24}$$

and $g(w)dw$ is normalized.

2.4.2 Anharmonicity

Generally, harmonic system assumes that the displacement of nuclei from their equilibrium position are small and thus, interatomic potential is truncated up to quadratic terms and the phonons frequencies thus derived does not explicitly depend on temperature or amplitude of their vibrations. Even though this approximation is valid for many solids at low temperature but tends to disagree as amplitude of vibration increases with temperature. So, at high temperature system or phase transistion, some fundamental properties like: thermal expansion are completely unaccounted by harmonic approximation, thus leading to infinite thermal conductivity in absence of phonon-phonon scattering. Also, force constant and elastic constant remains invariant with pressure or temperature.

Thus, if one considers the vibration of system in term of phonons, the small deviation from the harmonic case is a perturbation theory and the results is a shifting of phonon frequencies [50]

$$\widetilde{w}(\boldsymbol{qj}) = w(\boldsymbol{qj}) + \Delta(\boldsymbol{qj}) - i\Gamma(\boldsymbol{qj}) \tag{2.25}$$

Where, $\widetilde{w}(\boldsymbol{qj})$ is the renormalized frequency and $w(\boldsymbol{qj})$ *is* the frequency of mode $(\boldsymbol{qj})$. last term $\Gamma(\boldsymbol{qj})$ gives the phonon damping. For $\Gamma/_{w} << 1$, leads to weak anharmonicity. The shifted in phonon frequencies are typically measured using neutron scattering [50-53].

In case of one-dimensional oscillator, the potential including anharmonicity can be expressed as

$$V(x) = \frac{1}{2}Mw^2x^2 + V_3x^3 + V_4x^4 \tag{2.26}$$

If we consider $V_3 = V_4 = 0$, the system becomes harmonic with energy eigen state $E_n = (n + 1/2)\hbar w$, but taking account of third and fourth order in second-order perturbation gives the energy shift. *i.e.*,

$$\Delta E_n = \langle n|V_4x^4|n\rangle + \sum_{n'\neq n} \frac{|\langle n|V_3x^3+V_4x^4|n'\rangle|^2}{E_{n'}-E_n} \tag{2.27}$$

Since, $\langle n|V_3x^3|n\rangle$=0 as integrand is odd of x. And, the contribution of forth order of x is negligible in comparison to third order of x, so from last term, V_4x^4 can be neglected. Thus, the renormalized frequencies without damping can be written as:

$$\widetilde{w}(\boldsymbol{qj}) = w_0(\boldsymbol{qj}) + \Delta_2(\boldsymbol{qj}) + \Delta_3(\boldsymbol{qj}) + \Delta_4(\boldsymbol{qj}) \tag{2.28}$$

where, $w_0(\boldsymbol{qj})$ is harmonic frequencies considered at some reference temperature and volume. Δ_3 *and* Δ_4 are shift due to anharmonic potential, Δ_2 represents the softening of harmonic potential due to expansion and applied external pressure. The retaining of only Δ_2 in above equation represents the quasi-harmonic approximation.

Chapter 3: Quasi-Harmonic Approximation

3.1 Introduction and Methodology

The quasi-harmonic approximation (QHA) is a popular computational method which is often used to evaluate the thermal properties of materials [10] employing ab-initio simulations. In QHA, while employing quasi-harmonic model, phonon frequencies becomes volume dependent which leads to shift of minimum of free energy curve thus causing thermal expansion. The advantage of the method is that quantities such an internal energy and phonon frequencies are evaluated at zero temperature and thus requires only electronic relaxation. Because of this, it is widely used in evaluating the equation state (EOS) of a large number of materials.

In QHA, vibrational free energy is given by

$$F_{vib}(V,T) = \frac{1}{N_K} K_B T \sum_{\boldsymbol{k},n} ln\left[2\sinh\left(\frac{\hbar w_{n,\boldsymbol{k}}(V)}{2K_B T}\right)\right] \tag{3.1}$$

where, phonon frequency ($\omega_{n,k}(V)$) is only volume dependent as the temperature dependent intrinsic phonon interaction has been neglected and, entropy is given as

$$S(V) = -\frac{1}{N}\sum_{\boldsymbol{k},n} K_B ln\left[1 - exp\left(-\frac{\hbar\omega_{n,\boldsymbol{k}}}{K_B T}\right)\right] \tag{3.2}$$

$$+\frac{1}{N}\sum_{\boldsymbol{k},n} K_B \frac{\hbar\omega_{n,\boldsymbol{k}}(V)}{K_B T}\left[exp\left(\frac{\hbar\omega_{n,\boldsymbol{k}}}{K_B T}\right) - 1\right]^{-1}$$

3.1.1 Evaluation of Thermodynamic Quantities

Thermal Pressure

Determining the volume dependence of thermal pressure which is responsible for thermal expansion is a key tool to study the anharmonic behavior of any system. It represents the expansion

effect in a crystal that is caused by the atomic vibrations. The deviation of thermal pressure from linearity in thermal pressure versus temperature plot gives the measure of anharmonicy of the system. The Equation of state (EOS) for solid in thermodynamics is given as:

$$\mathrm{P_{total}(V,T)} = \mathrm{P(V,0)} + \gamma \frac{C_V \mathrm{T}}{\mathrm{V}} \tag{3.3a}$$

where, P_{tot} (V, T) is the total pressure, P (V, 0) is the pressure at given volume V at T=0K, γ is the Grüneisen parameter. Where,

$$P_{th} = -\frac{\partial F_{vib}}{\partial \mathrm{V}} = \left(\sum_{\boldsymbol{k},n} \frac{V}{w_{n,\boldsymbol{k}}} \frac{\partial w_{n,\boldsymbol{k}}}{\partial V}\right) \frac{T}{V} \left(K_B \left[\frac{\hbar w_{n,\boldsymbol{k}}(V)}{K_B T}\right]^2 \frac{e^{\hbar w_{n,\boldsymbol{k}}(V)/K_B T}}{\left[e^{\hbar w_{n,\boldsymbol{k}}(V)/K_B T} - 1\right]^2} \right) = \boldsymbol{\frac{\gamma C_V T}{V}} \tag{3.3b}$$

where, γ gives anharmonicity due to lattice vibration and E_{th} includes the anharmonicity due to atomic thermal vibration. Thermal pressure provides the information in understanding how temperature and pressure effects the behavior of solid (accounting Temperature). Models that properly reproduce thermal pressure are very important to accurately predict EOS.

Grüneisen parameter (γ)

Many properties of solids can be interpreted in terms of the harmonic approximation by considering the vibration of atoms as classical oscillator. But when it comes to high energy (high temperature), there is also no presence of thermal expansion in harmonic approximation thus many thermodynamical proprieties remains unexplained. And we need to include the anharmonicity in a system which gives a property of lattice vibrations and explain how well they interact and conduct heat. These properties can be characterized by a parameter called Grüneisen parameter which also gives the probability of phonon–phonon interactions and is proportional to γ^2.

Grüneisen parameter has both microscopic (mode Grüneisen parameter) and macroscopic (thermodynamical Grüneisen parameter) definition but the physical connection between them is still unclear. Macroscopic definition can be evaluated experimentally but microscopic definition is associated with vibrational frequencies of atoms in a solid.

Thermodynamic Grüneisen parameter

Thermodynamic Grüneisen parameter is calculated by equation of state fit. Thermodynamically, the Grüneisen parameter can be written as

$$\gamma_{th} = \mathrm{V}\left(\frac{\partial \mathrm{P}}{\partial \mathrm{E}}\right)_{\mathrm{V}} = \alpha \frac{\mathrm{B_T V}}{\mathrm{C_V}} = -\left(\frac{\partial \ln \mathrm{T}}{\partial \ln \mathrm{V}}\right)_{\mathrm{S}} = \frac{\mathrm{B_S}}{\mathrm{T}}\left(\frac{\partial \mathrm{T}}{\partial \mathrm{p}}\right)_{\mathrm{S}} \quad (3.4\ \mathrm{a})$$

where, V is the volume, C_V is heat capacity under constant volume, E is energy, α is the volume thermal expansion coefficient, and B is bulk modulus. This equation also gives the relationship between γ_{th} and α_V.

Similarly, the anharmonic contribution in Grüneisen parameter can be calculated using the entropy (S) from following relations:

Isochoric anharmonicity,

$$\gamma_{\mathrm{V}} = \left(\frac{\partial \ln \mathrm{S}}{\partial \ln \mathrm{V}}\right)_{\mathrm{T}} = \frac{V}{S}\left(\frac{\Delta S}{\Delta V}\right)_{T} \quad (3.4\ \mathrm{b})$$

And, Isothermal anharmonicity,

$$\gamma_{\mathrm{a}} = \left(\frac{\partial \ln \mathrm{S}}{\partial \ln \mathrm{T}}\right)_{\mathrm{V}} = \frac{T}{S}\left(\frac{\Delta S}{\Delta T}\right)_{v} \quad (3.4\ \mathrm{c})$$

Mode Grüneisen parameter

Microscopically, for cubic system, mode Grüneisen can be written as a logarithm volume derivative of the phonon frequency (i.e., using result of second (SOEC) and third order elastic constant (TOEC)).

$$\gamma_{\mathrm{n,k}} = -\left(\frac{\partial \ln w_{\mathrm{n,k}}}{\partial \ln V}\right)_{\mathrm{T}} \tag{3.5}$$

where, $\omega_{n,\,k}$ is the frequency of individual phonon at n-th mode of vibration is a function of wavevector (**k**) and V is the volume.

At low temperature limit, the vibrational Grüneisen parameter γ_{vib} is microscopic, quantum-mechanical approximation of γ_{th}, assuming that quasi-harmonic lattice dynamics is appropriate, and the normal mode phonon frequencies $\omega_{n,\,k}$ (V) are only volume dependent.

$$\gamma_{vib}(\mathrm{V,T}) = \frac{\sum_{n,k} \gamma_{n,\mathbf{k}}(V) C_{n,\mathbf{k}}(V,T)}{\sum_{n,\boldsymbol{k}} C_{n,\mathbf{k}}(V,T)} \tag{3.6}$$

$$C_{n,\boldsymbol{k}}(V,T) = \left[\frac{\hbar w_{n,\boldsymbol{k}}(V)}{K_B T}\right]^2 \frac{e^{\hbar w_{n,\boldsymbol{k}}(V)/K_B T}}{[e^{\hbar w_{n,\boldsymbol{k}}(V)/K_B T} - 1]^2} \tag{3.7}$$

where, $C_{n,\,k}$(V,T) is the heat capacity under constant volume for specific phonon modes (n, k). **k** is the wave vector and sum over normal modes is first Brillouin zone. Using QHA, at high temperature where the normal modes are fully thermally populated and C_v = 3NKB, it can be shown that vibrational Grüneisen is just simply average of normal mode Grüneisen parameter.

$$\gamma_{\mathrm{vib}}(\mathrm{V}) = \langle \gamma_{\mathrm{n,k}} \rangle \tag{3.8}$$

But, at low temperature ($T<T_D$) where low frequency modes dominate (i.e., normal mode frequencies $\omega_{n,k}(V)$ depend only on volume, not temperature so significantly Grüneisen parameter differ from its high temperature value.

Based on the continuum limit, for long-wavelength acoustic modes, we can express Grüneisen in terms of second and third-order elastic constants.

Several approximations have been developed over the years. The Slater [11], Dugdale and MacDonald [12], and Vashchenko and Zubarev [13] proposed three different models for Grüneisen parameter which can be represented by the single formula as

$$\gamma(V) = \frac{\left[\frac{B'(V)}{2} - \frac{t}{3}\right]}{\left[1 - \frac{2t}{3}\frac{P(V)}{B(V)}\right]} - \frac{1}{6} \qquad , \begin{cases} t = 0, & \text{Slater} \\ t = 1, & \text{Dugdale\_MacDonald} \\ t = 2, & \text{Vaschenko} - \text{Zubarev} \end{cases} \tag{3.9}$$

where $B_0(V)$ is pressure derivative of Bulk modulus B(V).

The volume derivative of γ directly relates the elastic and thermal properties of materials at high pressure and high temperature [14].

$$\left(\frac{\partial ln\gamma}{\partial lnV}\right)_T = \frac{\beta_T}{\beta}\left(\frac{\partial K_T}{\partial T}\right)_P - \frac{X_T}{\beta^2}\left(\frac{\partial \beta}{\partial T}\right)_P - (1 - X_T)\left[1 - \left(\frac{\partial B_S}{\partial P}\right)_T\right] \tag{3.10}$$

where, β is expansivity, B_T is isothermal bulk modulus. K_T is isothermal compressibility given as

$$K_T = \frac{1}{B_T} = \frac{1}{V}\left(\frac{\partial V}{\partial P}\right)_T \tag{3.11}$$

Depending on the validity of the different assumptions that were made for different materials, some of these models may not yield accurate results and application of these models to actual material may result in large variations in the calculate thermal pressure [15].

Expansion Coefficient

Generally, most of the metals expand on heating and contract on cooling. Expansion coefficient is the property of material which indicates the changes in its size due to change in temperature [11]. In QHA the free energy contribution is linear with respect to change in volume which leads to temperature dependent shift in minimum free energy curve leading to thermal expansion.

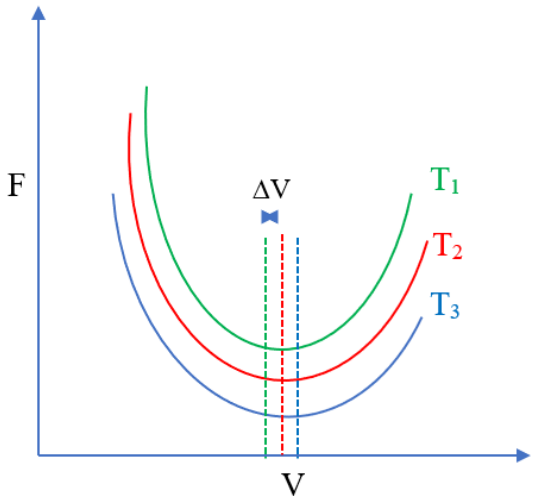

Figure 3.1: Schematic representation of free energy vs volume within QHA. ΔV represents the expansion due to shifting of minima at different temperature.

If the size of materials changes by lengthwise due to temperature, it is called linear thermal expansion and can be expressed as

$$\alpha_L = \frac{1}{L_0}\frac{dL}{dT} \tag{3.12}$$

where, dL is change in length due to change in temperature from T_0 to T_f.

Similarly, expansion coefficient in terms of volumetric change in material due to temperature is called volumetric expansion coefficient (α_V) and can be expressed as

$$\alpha_V = \frac{1}{V_0}\left(\frac{dV}{dT}\right)_p \tag{3.13}$$

where, V_0 is initial volume and dV is the change in volume due to change in temperature (dT). The subscript p indicates that pressure is kept constant during expansion of material. For isotropic materials, the relationship between α_L and α_V is given as

$$\alpha_V = 3\alpha_L \tag{3.14}$$

This factor 3 in this relation is because volume is composed of three mutually orthogonal directions.

The expansion coefficient is directly related to the anharmonicity of the solid and this can be explained by treating the atomic motions in terms of classical oscillators in an anharmonic potential, which can be written in term of atomic displacement x from their equilibrium separation at absolute zero as [8].

$$U(x) = cx^2 - gx^3 - fx^4 \tag{3.15}$$

where, c, g and f are parameters, x^3 represents the asymmetry of mutual repulsion between atoms and x^4 represents vibration softening at large amplitudes.

The average displacement can be calculated by using Boltzmann distribution function as

$$\langle x \rangle = \frac{\int_{-\infty}^{\infty} dx x \exp[-\beta U(x)]}{\int_{-\infty}^{\infty} dx \exp[-\beta U(x)]} \tag{3.16}$$

$$\langle x \rangle = \frac{3g}{4c2} k_B T \tag{3.17}$$

which shows that average displacement depends only on parameters c and g. Thus, we can say that in a system of classical oscillators, thermal expansion involves only antisymmetric terms gx^3. Even though this neglects symmetric term fx^4 but it still has a contribution in making the potential stable. In strongly bonded solid, ‘f’ will be higher so that thermal expansion is less but in weakly bonded solid, ‘f’ goes lower but ‘g’ goes higher thus expansion is more.

Chapter 4: Molecular Dynamics (MD) Methods

4.1 Introduction and Methodology

Molecular Dynamics (MD) is a computational method which is used to simulate the behavior of interacting system in a real time at finite temperature [11,12]. For classical particles, Molecular dynamics is governed by Newton's equation of motion but when the system is below Debye temperature, quantum mechanical approaches is used [13, 14]. Generally, classical MD integrates Equation of Motion (EOM) for any ensemble that is provided with initial position and velocities for finite time steps from which we can calculate various thermodynamic properties like: thermal expansion coefficient, phonon Density of state, etc. This method is applicable for all solids and liquids and even we can investigate effects of temperature in transition metals [15, 16].

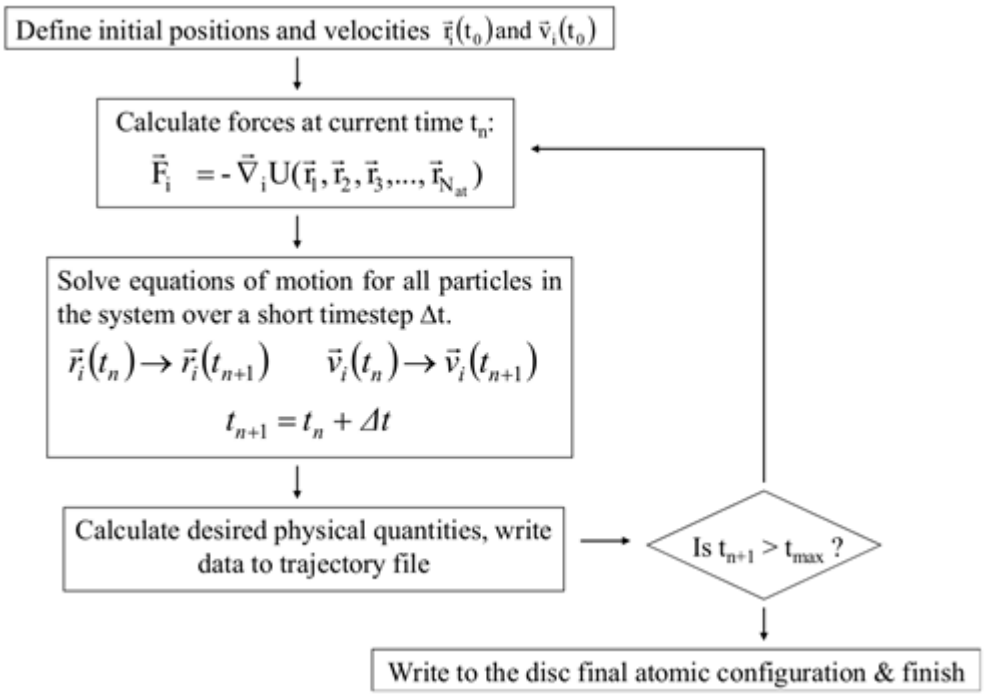

Figure 4.1: General scheme of MD simulation

In 1957, Alder and Wainright perform the first ever MD simulation considering the system of hard spheres to study the distribution of molecules in liquid [22]. In 1964, Rahman successfully solve the equation of motion using Lennard-Jones potential [23]. Several attempts were made to investigate the properties of materials using MD simulations which helps to develops this method rapidly. Then scientists extended this method from diatomic liquid to large molecules like proteins [24] with great accuracy in a result. Historically, Morse, Lennard-Jones and Born-Mayer potential are used in these situations but embedded atom model (EAM) are found to be more successful in metals. Since it is impossible to carry out "first principles" simulations using these potentials. In 1985, Car and Parinello introduced a new technique to solve the first principle simulations (Quantum MD Simulations) [16] in which, a fictitious lagrangian is defined for both electron and nuclei and solved simultaneously. This new technique brings significant improvement on solving quantum MD equations but computationally it is very expensive method.

4.1.1 Classical Lagrange and Hamiltonian Dynamics

If we consider the system of collection of particles in which conservative force is described by potential, then

$$m_i \ddot{r}_{i=} \boldsymbol{F}_i \tag{4.1}$$

where, m_i is the mass of particle and $\mathbf{r}_i$ its position at any time t and $\mathbf{F}_i$ is the force acting on particle i. In above equation, left hand side of this equation is kinetic energy function and given as time derivative of momentum and right-hand side is force and given as derivative of potential energy as U is independent of temperature.

Then, for conservative system, the Lagrangian L=T-U, which is now function of both coordinates and velocities. Now, under variational approach we can establish

$$\frac{d}{dt}\left(\frac{\partial L}{\partial \dot{\boldsymbol{r}}_i}\right) - \frac{\partial L}{\partial \boldsymbol{r_i}} = 0 \tag{4.2}$$

The above equation is called Euler-Lagrange equation and under initial condition, the solution of this equation gives the trajectory of the system. If m is a mass of atom I, then for cartesian coordinate system,

$$\frac{\partial L}{\partial \boldsymbol{r_i}} = -\frac{\partial V}{\partial \boldsymbol{r_i}} \tag{4.3}$$

$$\frac{\partial L}{\partial \boldsymbol{r_i}} = -\frac{\partial V}{\partial \boldsymbol{r_i}} = -\Delta_{\boldsymbol{r}_i} V = \boldsymbol{F}_i \tag{4.4}$$

$$\frac{d}{dt}\left(\frac{\partial L}{\partial \dot{\boldsymbol{r}}_i}\right) - \frac{\partial L}{\partial \boldsymbol{r_i}} = m_i \ddot{r}_i - \boldsymbol{F}_i \tag{4.5}$$

Then, we define conjugate momentum ($\dot{p}_i$) and kinetic energy (T) as

$$\dot{\boldsymbol{p}}_i = \frac{\partial L}{\partial \boldsymbol{r_i}} \tag{4.6}$$

$$T = \sum_i^N \frac{\boldsymbol{p}_i^2}{2m_i} \tag{4.7}$$

For Hamiltonian dynamics, we define the system in terms of generalized coordinates and generalized momentum which is time independent for isolated system. The Hamiltonian of any system gives the total energy of that system. Mathematically,

$$H(\mathbf{p}, \mathbf{q}) = \sum_i^N \frac{\mathbf{p_i}^2}{2m_i} + V(\mathbf{q_1}, \ldots, \mathbf{q_N}) \tag{4.8}$$

and in terms of Lagrangian, H can be written as

$$H(\mathbf{p}, \mathbf{q}) = \sum_i \mathbf{p_i} \dot{q}_i - L(\mathbf{q}, \dot{\mathbf{q}}) \tag{4.9}$$

where, $\dot{p}_i = \frac{\partial L}{\partial\, \dot{q}_i}$ is a canonical momentum and,

$$\dot{\mathbf{q}}_\mathbf{i} = \frac{\partial H}{\partial \mathbf{p_i}} \tag{4.10}$$

$$\dot{\mathbf{p}}_\mathbf{i} = -\frac{\partial H}{\partial \mathbf{q_i}} \tag{4.11}$$

4.10 and 4.11 are the Hamiltonian equations and gives the equation of motion of a given system.

4.2 How macroscopic properties can be extracted from the Molecular Dynamics?

Statistical mechanics plays vital role in connecting the computer-generated microscopic information with the macroscopic information in terms of energy, pressure, etc. If there are large number of particles in an isolated system (constant energy E), then fluctuations in a system must fluctuate about a constant energy. Thus, experimentally observed macroscopic property of a system is given by the time average taken for a long- and finite-time interval. However, statistical mechanics use the concept of 'ensemble average' [22] rather than time interval approach. The time evolution of a coordinates in a phase space (ensemble average, position or momentum of particle trajectories) gives the information of a system on the basis of statistical mechanics. For stationary ensemble which is explicitly time independent, the calculated average value of any physical quantity (for isolated system, it is energy), is also time independent. Clearly, such ensemble represents equilibrium system. For an isolated system with constant number of particle N and energy E, restricted in a fixed volume V, thermodynamic states can be determined using these extensive variables (N, V and E). This type if system/ensemble is called micro-canonical (NVE) ensemble.

4.3 ENSEMBLES

An ensemble is a collection of a large number of microscopically identical but essentially independent systems. On the basis of interaction of the system with the surroundings an ensemble is classified into three types.; microcanonical (NVE), canonical (NVT) and isobaric-isothermal (NPT) ensemble. For each ensemble, given extensive variables are kept fixed. The averages produced by ensembles are consistent if they are in same state of a system. However, in real phenomena, such average deviates from equilibrium causing fluctuation which varies in different ensemble. These averages or fluctuation used to calculate different structural, energetic and dynamic properties over ensemble generated.

4.3.1 Microcanonical (NVE) Ensembles

It is an isolated system. *i.e.,* this system the total energy and volume are preserved whereas the temperature and pressure are fluctuating and obtained directly by solving Newton's equation without controlling temperature and pressure. Since energy is assumed to be con served when we generate this type of ensemble but we can notice a slight change in energy due to rounding and truncation errors during the integration process. Thus constant-energy simulations are not recommended for equilibration because without energy flow, desired temperature cannot be obtained. In the NVE ensemble, the Hamiltonian and equations of motion are given as

$$\mathbf{H} = \sum_{i=1}^{N} \frac{\mathbf{p_i}^2}{2m_i} + V(\mathbf{r_i}) \tag{4.12}$$

$$\dot{\mathbf{r}}_\mathbf{i} = \frac{\partial \mathbf{H}}{\partial \mathbf{p_i}} \dot{\mathbf{p}}_\mathbf{i} = -\frac{\partial \mathbf{H}}{\partial \mathbf{r_i}} \tag{4.13}$$

4.3.2 Canonical (NVT) Ensembles

In this ensemble number of particles, statistical temperature and total volume of a system is kept constant but energy of each cell fluctuates. Temperature is controlled directly through temperature scale during initialization stage and through temperature-bath coupling during data collection phase. In practice, true canonical ensemble can be produced by using the Nose-Hoover method [20, 21] which is similar to the extended Lagrange method. The partition function Q for NVT ensemble is given as

$$Q = \frac{1}{N!h^{3N}} \int_{-\infty}^{\infty} \int_{D(V)} d\mathbf{r^N}\, d\mathbf{p^N} exp[-\beta H(\mathbf{r^N}, \mathbf{p^N})] \tag{4.14}$$

On NVT ensemble, free energy A = U−TS is minimum at equilibrium and $\beta = 1/K_BT$ is the statistical mechanical temperature. Since, NVT ensemble has no coupling to a pressure bath provides advantage of less perturbation of the trajectory.

4.3.3 Isobaric-Isothermal (NPT) Ensembles

The number of particles is fixed and ensemble is maintained at constant pressure and temperature due to which volume of a system changes depending on the internal pressure. NPT system has heat baths and “barostats”. The temperature is kept constant using heat bath and the pressure is controlled by coupling to a pressure bath. The partition function (Δ) for NPT ensemble is given as:

$$\Delta = \frac{1}{V_0 N!\, h^{3N}} \int_0^{\infty} \int_{-\infty}^{\infty} \int_{D(V)} d\mathbf{r^N}\, d\mathbf{p^N} dV exp[-\beta H(\mathbf{r^N}, \mathbf{p^N}) - \beta P v] \tag{4.15}$$

where, P is the external pressure applied on a system of volume V and with Gibbs free energy G = U−TS+PV minimized at equilibrium. This ensemble is considered important when pressure, volume and densities are most important in the simulation. Furthermore, during

equilibration, we can use this ensemble to obtain desired pressure and temperature before changing our ensemble to constant-energy or constant-volume ensemble.

4.4 INTER-ATOMIC INTERACTIONS

Different models have been evolved for calculating interactions between atoms in MD simulations and these methods have been improved over time. In the beginning, Lennard-Jones potential was popular to calculate the properties of material using MD. LJ interaction model is a pairwise additive force model and neglects the changes in local electron density. However, metallic crystal shared valance electrons with neighboring ions. Thus, the inter-atomic interaction in metals is mostly affected when there is change in local electron density and the inter-atomic interactions takes the account of local electron density. So, this method is considered more accurate. However, all these methods are based on different physical arguments (tight binding model, effective medium theory, etc.). Some of these models which are based on many body effects are

- Embedded Atom Method (EAM) [22, 23, 24]
- Finnis Sinclair [30]
- Glue Model [31]

Later, quantum-based interatomic potentials using tight binding theory [26, 27] and generalized pseudopotential theory [34] including angular force contributions were developed.

4.4.1 Embedded Atom Method (EAM)

EAM is Density Functional Theory (DFT) based semi-empirical radial-force method, where the energy of any structural arrangement of nuclei (potential energy) is a function of the positions of the atoms as well as the local electron density. Since, this method is economic and can

describe the mechanical properties of metals so it is widely used for large scale atomic simulations of metallic crystals. In this method, each atom is assumed to be influenced by locally uniform electron gas of neighboring atoms. The energy that is required to embed the central atom in to this electron cloud is then calculated which is sum of potential energy of each individual atoms (E_i).

$$E_{tot} = \sum_{i}^{N} E_i \tag{4.16}$$

and, potential energy per atom i is given by

$$E_i = F(\bar{\rho}_i) + \frac{1}{2}\sum_{i \neq j} \phi(r_{ij}) \tag{4.17}$$

where, $F(\bar{\rho}_i)$ is the energy required for atom i to embedded into electron gas of density ρ_i and $\phi(\mathbf{r}_{ij})$ is a pair-wise (short-range) potential between atom i and neighbor atom j at distance $\mathbf{r}_{ij}$. Where electron density function $(\bar{\rho}_i)$ is given as

$$\bar{\rho}_i = \sum_{j \neq i} f(r_{ij}) \tag{4.18}$$

where, f is a spherically symmetric function.

Since, EAM assumes that electron density of metallic iron is spherically symmetric due to which mechanical properties of partially filled d block metals cannot be predicted by EAM. However, Ravelo et al. [35] shows that under shock loading, mechanical properties of bcc Ta can be predicted by careful selection of high-pressure properties in training set.

EAM Model Potentials for Tantalum

Ravelo et al. [35] developed two different EAM model potentials (Ta1, and Ta2) for tantalum which are evaluated by comparing simulated Hugoniot elastic limit (HEL), melt curve, and defect structures under shock compression with experimental data. These potential models

have been widely used in computational studies to investigate mechanical properties of Tantalum. There is slight differences between these two potentials models which is assumed to be present due to different descriptors used as training set. Thus, Ta2 is assumed to represent thermal pressures more accurate than Ta1.

Table 4.1: Parameters of the EAM function of Ta2 potential.

Parameter	Ta2
E_c (eV)	8.1
α	4.95
a_0 (Å)	3.304
f_3	-0.035744
f_4	-0.020879
U_0 (eV)	1.1094
r_1 (Å)	2.7826
α_P	4.6463
β_3	0.160
β_4	0.060
r_s (Å)	2.8683
s	8.00
r_c (Å)	5.5819
a_1 ($Å^{-s}$)	-0.039742
a_2 ($Å^{-(s+1)}$)	0.038568
a_3 ($Å^{-(s+2)}$)	-0.012714
a_4 ($Å^{-(s+3)}$)	0.0014196
p	5.9913
q	8.0
ρ_0	0.074870

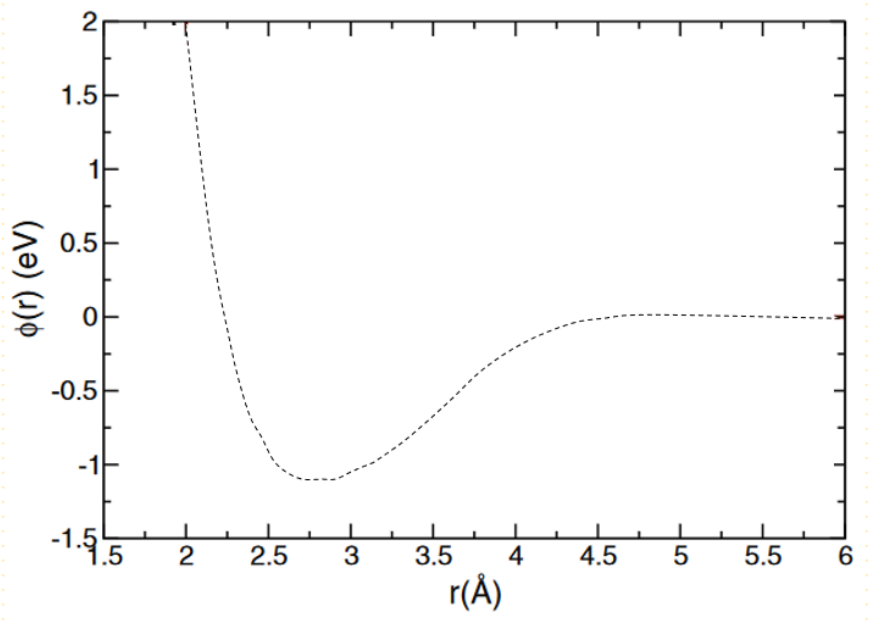

Figure 4.2: Potential functions of the EAM models Ta2.

4.5 ADIABATIC SWITCHING

The thermal properties such as entropy and free energy are very difficult to compute because they cannot be expressed in terms of ensemble averages. Entropy gives the information in overall state of order of the system in phase space. The entropy of a crystal (S_{MD}) is composed of the quasi-harmonic term (S_H), the anharmonic term (ΔS). The combination of QHA and MD entropy allows us to make an accurate determination of the anharmonic entropy of transition metals.

$$\Delta S = S_{MD} - S_H \tag{4.19}$$

The analysis of entropy can also be accomplished by using phonon dispersion curves, using neutron-scattering experiments, which gives the value characteristic temperature, thus harmonic

entropy, the anharmonic entropy can be obtained without assumption about its magnitude or temperature dependence.

$$S_H = 3\left[ln\left(\frac{T}{\Theta_0}\right) + 1 + \frac{1}{40}\left(\frac{\Theta_1}{T}\right)^2 + \ldots..\right] \tag{4.20}$$

The vibrational entropy (S_H) increases with phase space (i.e., temperature). For short time scales, entropy can be related to the mean square displacement ($< U^2 >$) which signifies the space available for particles in a system to fluctuate. Generally, entropies of any system are calculated via the density of states (DOS)which provides a best way of counting microscopic states of the given system.

$$S_H = K_B \sum_{i}^{3N} ln\omega_i \tag{4.21}$$

In the present work, entropy differences as functions of temperature is calculated using adiabatic switching using MD formalism. Unlike QHA, this method is not restricted to low temperatures and is thus applicable over a wider temperature range. The adiabatic switching method is based on Kirkwood's idea [36] to connect the model system with reference system whose free energy is known .The effective Hamiltonian for both systems is written as:

$$H_{eff} = (1-\lambda)H_0 + \lambda H_{ref} = H_0 + \lambda\Delta H \tag{4.22}$$

H_0 is the Hamiltonian of known system and H_{ref}, the Hamiltonian of the reference system. In determining free energy of a solid, the reference system is usually taken to be an Einstein (harmonic) solid, i.e. each atom in the system is an independent harmonic oscillator. and $0 \leq \lambda \leq 1$. Thus, free energy difference of system is:

$$\Delta F = F_{MD} - F_0 = \int_0^1 \frac{\partial H_{eff}(\lambda)}{\partial \lambda} d\lambda = \int_0^1 \langle \Delta H \rangle_\lambda d\lambda \tag{4.23}$$

< > is MD time averaging and path from λ=0 to λ=1 is reversible. This approach has drawback that several simulations for different values of l are required to evaluate the value of integral. Watanabe and Reinhardt [37] suggested the integral be carried out dynamically by allowing the value of λ to be a function of time.

For harmonic system, the internal energy (E_{ref}) and Free energy (F_{ref}) is given as:

$$E_{ref} = \phi_{ref} + 3K_BT \tag{4.24}$$

and,

$$F_{ref} = \phi_{ref} + 3K_BTln\left(\frac{\hbar w}{K_BT}\right) \tag{4.25}$$

Where, $\emptyset_0$ is the value of 0K potential for harmonic crystal, $w = \sqrt{\frac{k}{m}}$ is the frequency of harmonic solid, k is spring constant and m is atomic mass of the given solid.

According to thermodynamics, the entropy of Einstein solid (S_{ref}) is:

$$S_{ref} = \frac{F_{ref} - E_{ref}}{T} = 3\left[1 + ln\left(\frac{K_BT}{\hbar w}\right)\right] \tag{4.26}$$

The entropy difference between 2 system is measures the given as:

$$\Delta S = \left(\frac{(E_{ref} - E_0) - \Delta F}{T}\right) \tag{4.27}$$

using $\Delta S = S_{ref} - S_0$, the above equation becomes,

$$S_{ref} - S_0 = \left(\frac{\phi_{ref} + 3K_BT - E_0 - \Delta F}{K_BT}\right)$$

$$S_0\,(V,T) = \; S_{ref} - \left(\frac{\phi_{ref} + 3K_BT - E_0 - \Delta F}{K_BT}\right) \tag{4.28}$$

where, $S_{ref}\,(V,T)$ is the entropy of the model under constant volume, at given temperature.

In recent years, more accurate phonon data are available for many elements which are calculated from neutron scattering experiments. These data allow us to make accurate calculations

of the quasi-harmonic entropy. With this information, the anharmonic entropy can be calculated from the total measured entropy of the given system. This procedure is does not invoke anharmonic perturbation theory; indeed, there is no restriction on the magnitude or temperature dependence of S_A [38].

4.6 STATISTICAL UNCERTAINTIES IN SIMULATIONS

MD simulation is a statistical method and thus the results obtained are statistical averages [39] and to compare these data to experimental data, one need to make sure that the data obtained from MD simulations are precise. So, we need to take account of errors that can be occurred during MD simulations. There are two kinds of errors that can occur statistical and systematic [39].

Statistical error can be identified by calculating standard deviation of obtained statistical MD data. Lower the standard deviation, more precise the data and vice versa. Also, standard deviation depends on duration of simulation of data. Thus, running the simulation for longer time will helps in decreasing the statistical errors. Systematic errors are very hard to recognize and may not decreases with time duration of simulation. It can be minimized by increasing the number of atoms in the system due to less influence of boundary conditions [39]. Furthermore, we can check systematic errors by comparing our MD data with other different simulation methods.

4.7 DATA ANALYSIS

All the information that molecular dynamics simulation gives, can be extracted from the trajectories of the particles. We need to discarded a fair number of time steps before the system attains equilibrium state. To determine whether the system reached equilibrium or not, we can look

at change in total energy with time. We can also determine the equilibrium by velocity distribution function also.

Since, the atoms are always vibrating around their equilibrium positions, the calculation of time average of position gives accurate lattice parameters. Also, we can obtain some thermodynamic properties by taking derivative from a set of different environments. For example, the we can obtain bulk modulus by running under NVE taking a few different volumes, and comparing the calculated pressures. We can also do the same for the thermal expansion coefficient.

We wish to obtain information about phonon dynamics from these trajectories. For this, we run a simulation of sufficient size and time step and run for long enough time using interatomic potentials. The temperature dependence of vibrational spectrum from trajectories can be obtained from velocity autocorrelation function. Autocorrelation function helps to obtain clear signal wit clear period as it removes the noise from the signal.

Chapter 5: Results and Comparisons

In this chapter, we briefly discuss all the steps that we used to calculate the properties of tantalum at different temperature. We will also explain how we obtain different thermal properties and other properties like: Root Mean Square Displacement (RMSD), entropy difference for tantalum using MD simulation. We used the preexisting md11h and md12h codes for MD simulations.

5.1 COMPUTATIONAL DETAILS

5.1.1 Creating the input and Performing MD simulations

We begin with defining the input parameters for which we want to run our calculations. This includes three main things. First, we need a sample of tantalum for which we want to study its thermal properties. In order to minimize statistical uncertainties during simulations, we choose a sample that is as big as possible as this would provide more discrete values of the wave vectors but also size of the sample affects the speed of the calculations which grows with number of atoms. So, we choose a sample containing 5500 atoms arranged approximately in a 14x14x14 cube. We used Embedded atom method (EAM) potential for Ta which reproduce EOS for each material.

Since we are interested in temperature dependence of phonon, so temperature is second parameter to be considered. Since performing MD simulations is impossible at 0K, thus we choose to perform simulation between 100K to 3000K temperature. While creating the sample it is necessary to know that the lattice parameter is temperature dependent. Thus, setting P = 0, could find the equilibrium area of the sample at a given temperature. We have performed the MD simulation at 0 GPa and 50 GPa pressure.

We calculate the trajectories and velocities of each atom in a system. We chose time steps $\Delta t=0.01$ and we save the results every 10 timesteps in order to reduce the amount of memory space

we use. We choose a total N=20,000-time steps. Md11h and md12h code is used to run the MD simulations. The shaded region in the plots indicates the region below Debye temperature (246 K for Ta). The temperature range for our calculation lies from 100K to 3000K.

5.2 Results

5.2.1 Expansion Coefficient

We performed constant pressure temperature (NPT) simulation and used eq. 3.13 calculate thermal expansion coefficient of Tantalum at 0 pressure. To study the effects of pressure on thermal expansion, we also performed simulations at 50 GPa pressure. The volumetric thermal expansion coefficient of the Tantalum as a function of temperature obtained using MD along with the Cohen and Gulseren [4] and experimental data [40] are presented (figure 5.1 and figure 5.2). Expansion coefficient via QHA is calculated by minimization of free energy at different temperature.

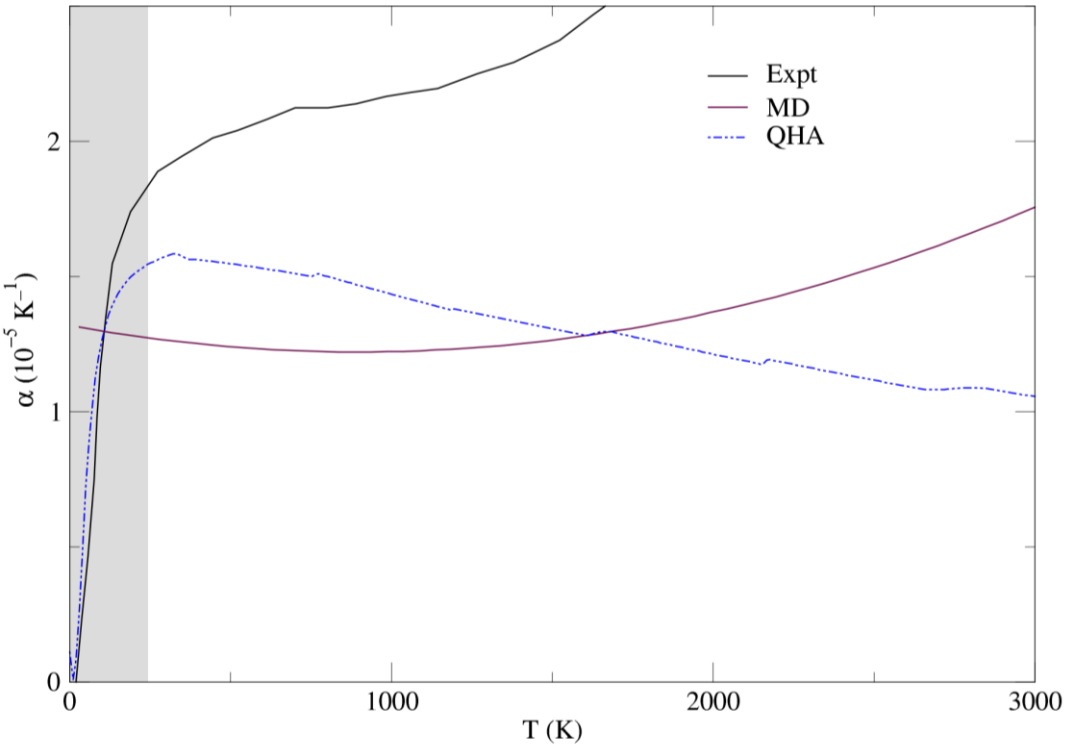

Figure 5.1: Calculated temperature dependence of the thermal expansion coefficient (TEC) of tantalum at 0 GPa pressure. Solid black line represents experimental value, Maroon dashed line represents the TEC calculated using QHA, and red line is the classical value of TEC calculated using MD.

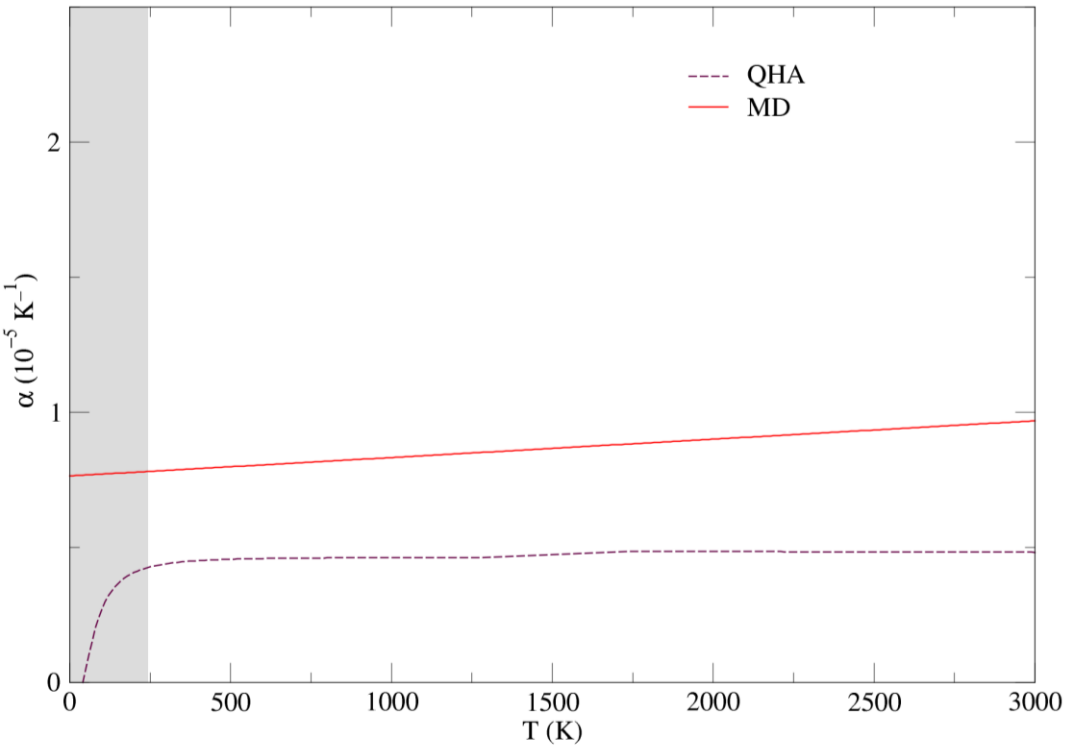

Figure 5.2: Calculated temperature dependence of the thermal expansion coefficient (TEC) of tantalum at 50 GPa pressure. Solid black line represents experimental value, Maroon dashed line represents the TEC calculated using QHA, and red line is the classical value of TEC calculated using MD.

It is seen that, when the pressure in the system increases, the pressure dependence on expansion coefficient decreases, which is in good agreement with the property of condensed materials. At high pressure, the effect of temperature on thermal expansion coefficient is very weak and can be neglected because the increase in pressure of system decreases the volume due to which depth of potential well increases thus reducing the anharmonic nature of the system.

The variation of volume with temperature (figure 5.3 and figure 5.4) shows that the volume expansion rate is almost same at 0 GPa calculation, which suggest that volume contribution is almost same, whereas the temperature contribution is dominating at low pressure. But in 50 GPa

regime, the volume expansion rate is faster in MD than QHA, which suggest that volume contribution is dominating at high pressure.

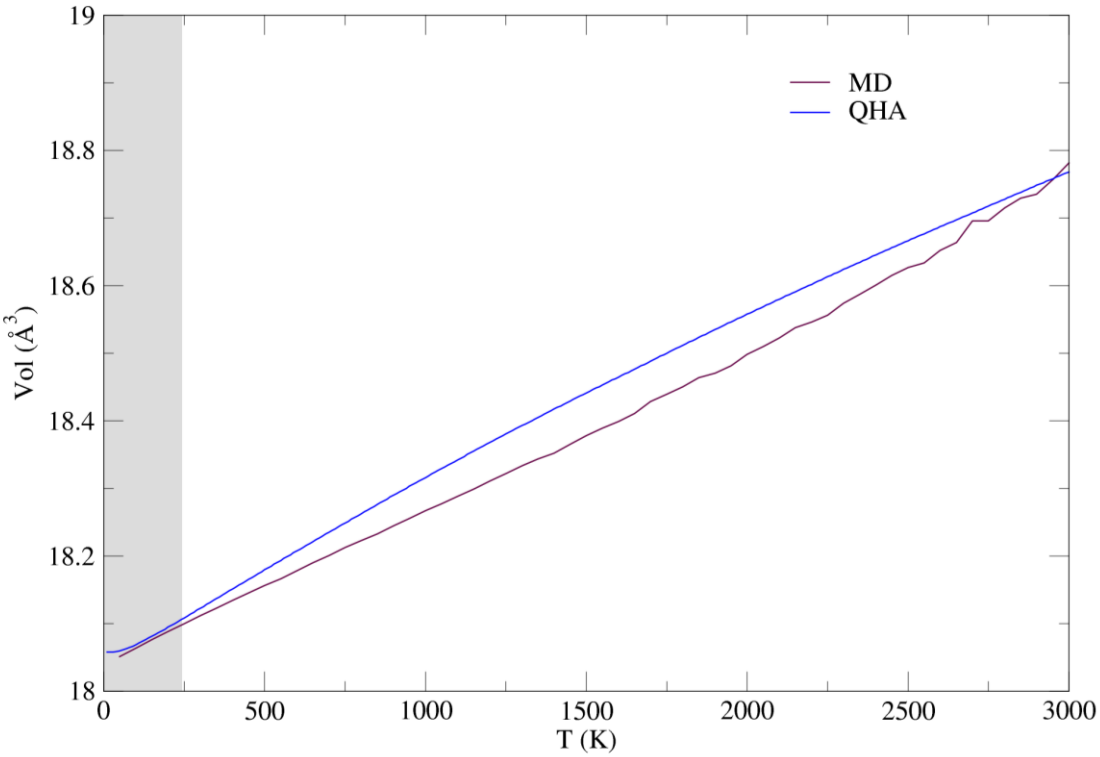

Figure 5.3: Atomic volume as a function of temperature for tantalum at pressure 0 GPa.

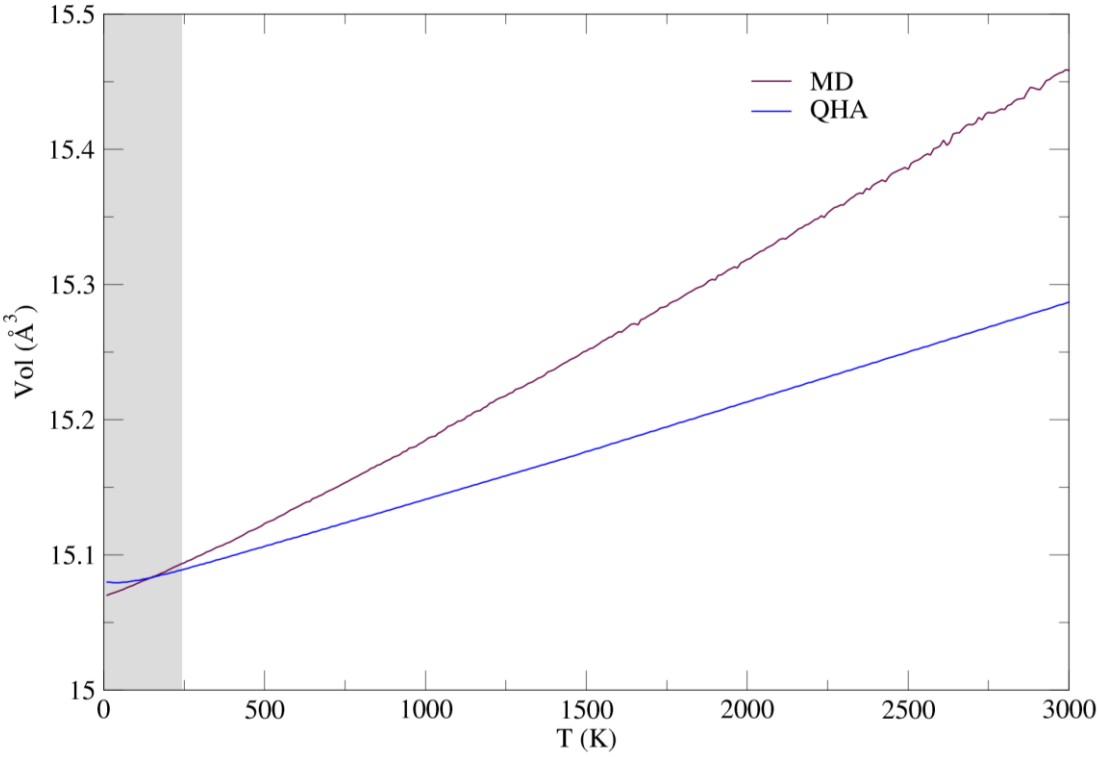

Figure 5.4: Atomic volume as a function of temperature for tantalum at pressure 50 GPa.

5.2.2 Grüneisen Parameter

Grűneisen parameter gives the measure of degree of anharmonicity. So, the calculation of the Grüneisen parameter is very important to predicts the anharmonic thermodynamic properties of solids. We first performed CMD simulation at constant pressure and temperature (NPT) to get the correct volume at given temperature. Finally, we run simulation considering NVT ensemble at different pressure. The variation of Grüneisen parameter as a function of temperature (figure 5.5 and figure 5.6) is evaluated using eq. 3.4a for MD and eq. 3.5 for QHA.

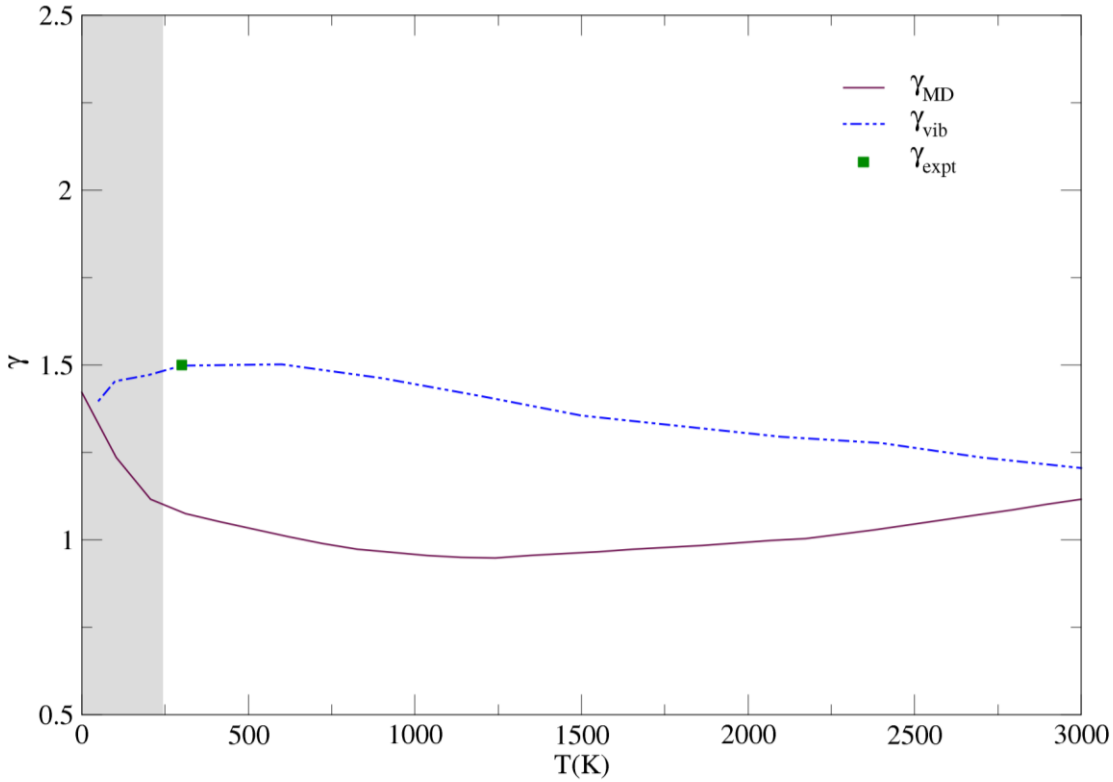

Figure 5.5: Variation of Grüneisen parameter with temperature at zero pressure. Blue dashed line represents the vibrational Grüneisen parameter calculated using QHA, and marron line is the classical value of Grüneisen parameter calculated using MD and the green square dot is the experimental value of γ at 0 GPa, 300K.

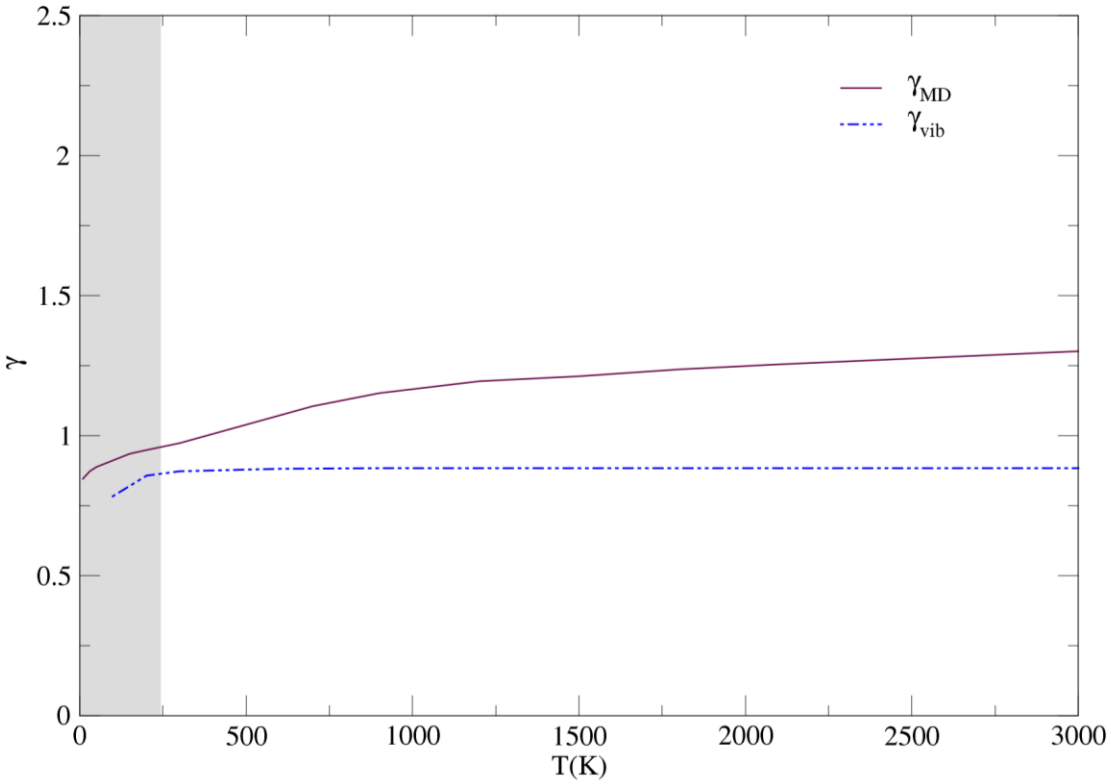

Figure 5.6: Variation of Grüneisen parameter with temperature at 50 GPa pressure. Blue dashed line represents the vibrational Grüneisen parameter calculated using QHA, and marron line is the classical value of Grüneisen parameter calculated using MD.

The experimental zero-pressure room temperature value of the Grüneisen parameter is 1.65. We see that Grüneisen parameter shows very less variation with change in temperature of the system. The higher pressure Grüneisen parameter at high temperature seems to be an overestimated in MD. The overestimation of at high temperatures could be attributed to the equation not accounting not accounting for the softening or decrease of Bulk modulus with temperature. Since, QHA doesn't take account of temperature so the vibrational Grüneisen parameter can be corrected by taking temperature dependence of phonon frequencies, which will be discussed later in section 5.2.3.

5.2.3 Free Energy and Entropy

We have calculated the free energy and entropy using adiabatic switching method in MD formalism, which is based on the facts that only one switching trajectory is enough to obtain the important information of the system. Using the path over switching to a harmonic solid has advantages as one can obtain the high accuracy result for relatively shorter switching times as well as a reduction in the number of switching runs since we do not require separate calculation for the free energy of the model solid and reference solid. The results obtained from adiabatic switching procedures using MD allow to determine the Helmholtz free energies which is very important in determining the free energy of real solid, thus entropy of the system.

Before we calculate any entropic contribution, we confirmed that, the different value of frequencies (spring constant K) at any given temperature produces the almost same value of entropy difference (anharmonicity). (figure 5.7). So, taking frequency contribution is not a big problem during switching method.

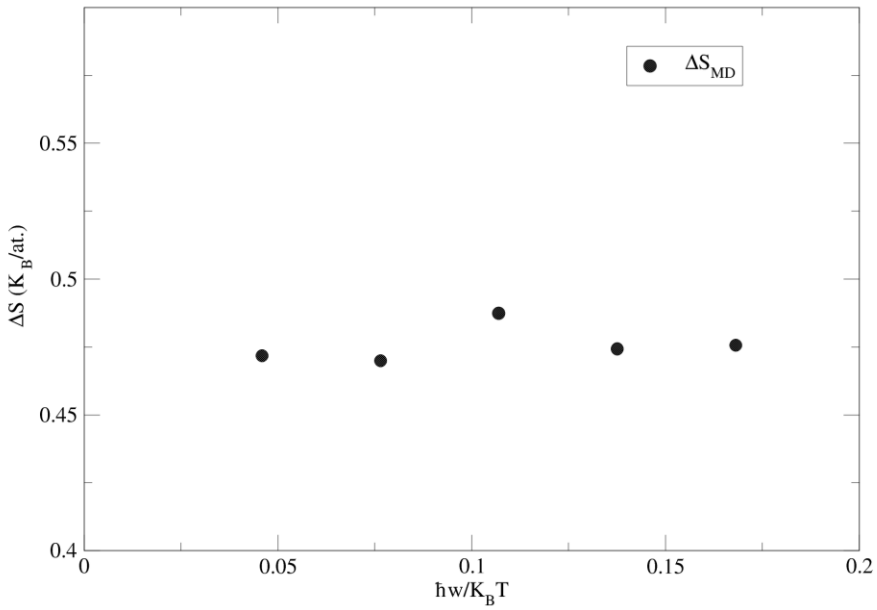

Figure 5.7: Entropy difference between MD and QHA (0 GPa, 1000K) measured as a function of frequencies.

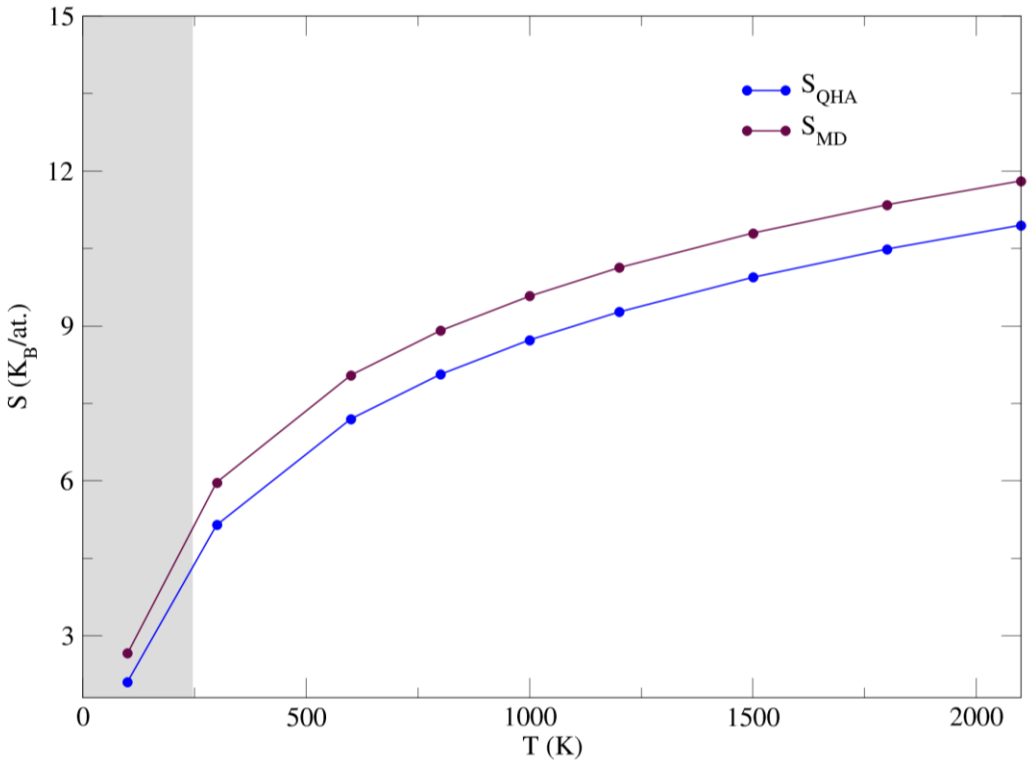

Figure 5.8: Temperature dependence of entropy calculated from NVT simulations at 0 GPa. Maroon line represents the entropy of model solid calculated via adiabatic switching and blue line is entropy calculated from quasi-harmonic approximation.

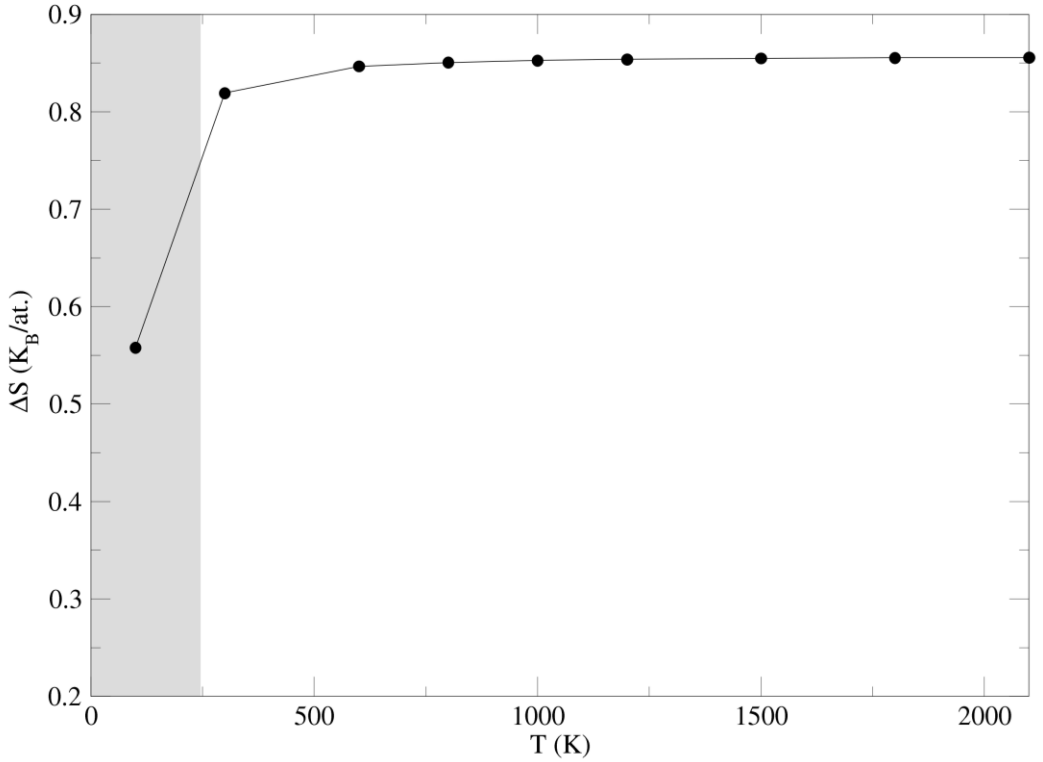

Figure 5.9: Temperature dependence of entropy difference between MD and QHA (anharmonicity) calculated at 0 GPa pressure.

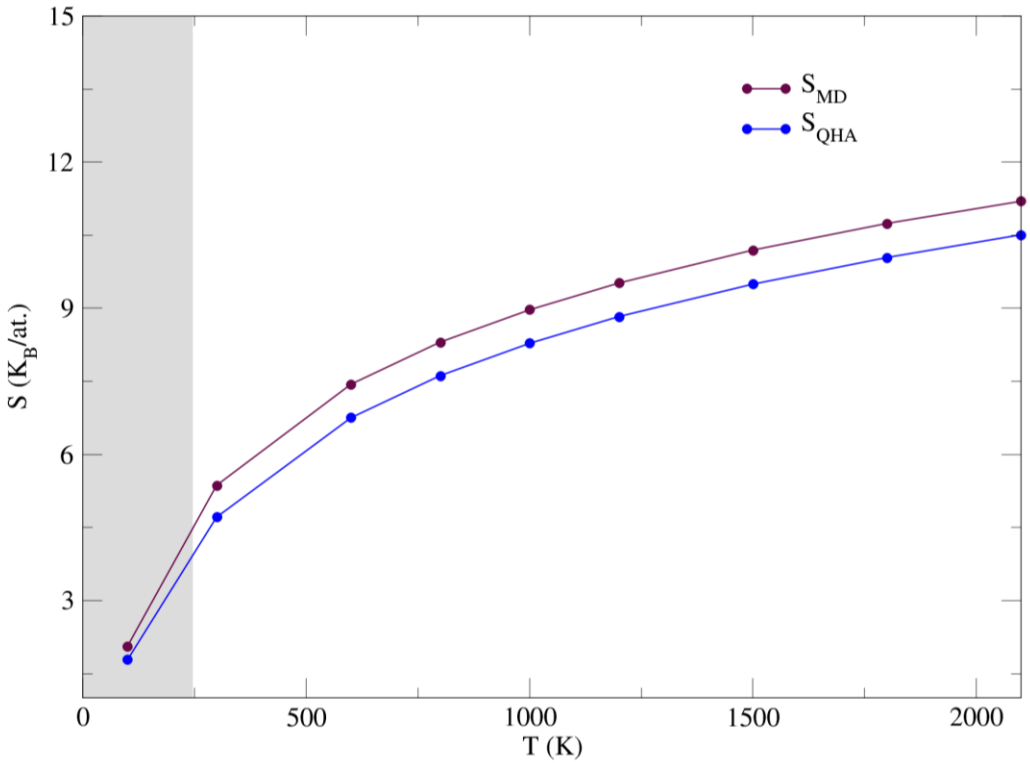

Figure 5.10: Temperature dependence of entropy calculated from NVT simulations at 50 GPa. Maroon line represents the entropy of model solid calculated via adiabatic switching and blue line is entropy calculated from quasi-harmonic approximation.

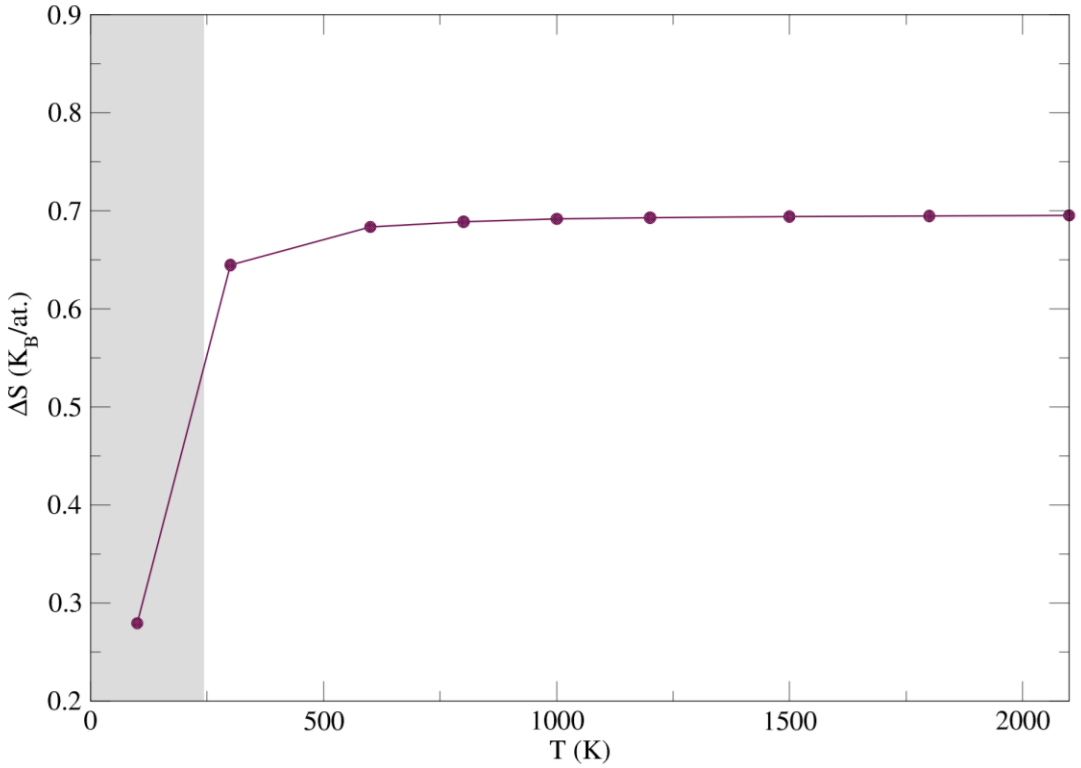

Figure 5.11: Temperature dependence of entropy difference between MD and QHA (anharmonicity) calculated at 50 GPa pressure.

The switching runs using MD simulations were performed at constant volume and temperature (NVT) at pressure 0 GPa and 50 GPa. The entropy (figure 5.8 and figure 5.10) calculated using MD (switching method) is higher than QHA calculation at all sampled temperatures. The difference between the *true* entropy of a model system (S_{MD}) and its QH estimate (S_{QH}) arises from anharmonicity. Thus, the entropy difference ($\Delta S = S_A = S_{QH} - S_{MD}$) as a function of temperature (figure 5.9 and figure 5.11) obtained from adiabatic switching process gives the measure of anharmonicity. It is found that the entropy differences increasing dramatically at low temperature which indicates the very high anharmonic contribution in a system. The flattening of curve at high temperature signifies that volume and temperature effects on the phonon energies are nearly equal and opposite at high temperature.

We have also calculated anharmonicity using RMS ($S_{a,rms}$), which shows that the volume contribution in anharmonicity increases sharply at low temperature and flatten at high temperature. But the comparison between thermal anharmonicity calculated form 0 GPa and 50 GPa entropy difference between MD and QHA ($S_{a,th}$)) and RMS ($S_{a,rms}$) (figure 5.12) shows that the volume contribution in anharmonicity is dominant at higher temperature regime and temperature contribution at lower temperature regime.

$$S_{a,rms} = 3K_B ln\left(\frac{u_{rms(0)}}{u_{rms(50)}}\right)$$

Where, $u_{rms(0)}$ is the RMS of particles at 0 GPa pressure and $u_{rms(50)}$ at 50 GPa pressure respectively.

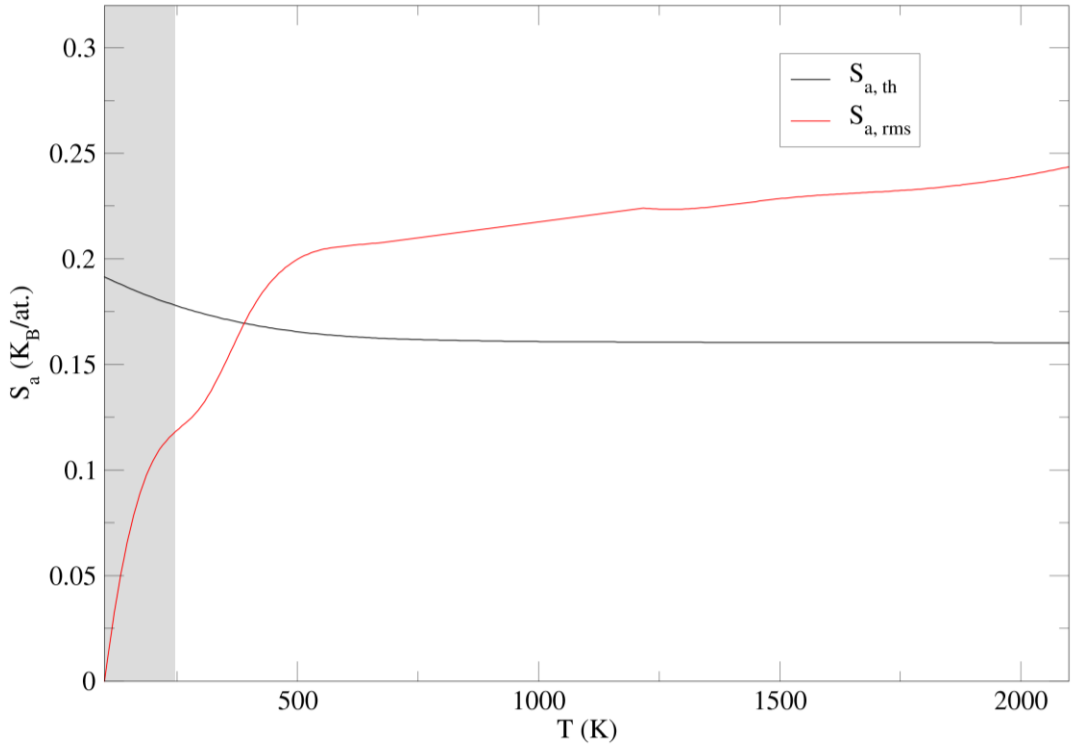

Figure 5.12: Comparisons between 0 GPa and 50 GPa entropy difference (anharmonicity) from MD using adiabatic switching (black solid line) and RMS (red solid line).

5.2.4 Some other thermodynamical properties

Thermal pressure

The deviation of thermal pressure from linearity in thermal pressure versus temperature plot gives the measure of anharmonicy. We have calculated thermal pressure using eqn 3.3b. The plot of thermal pressure versus temperature is shown below (figure 5.13 and figure 5.14).

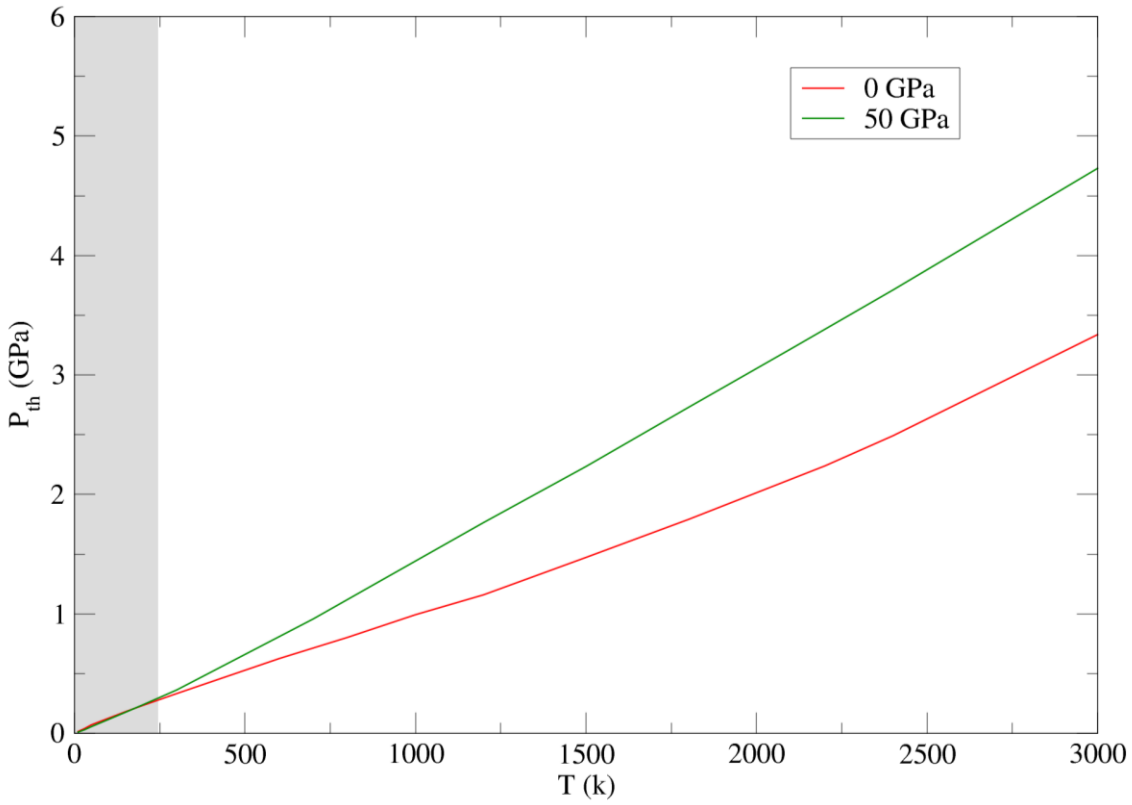

Figure 5.13: Temperature dependence of thermal pressure using MD. Green line styles correspond to 50 GPa calculation and red line representation 0 GPa calculation.

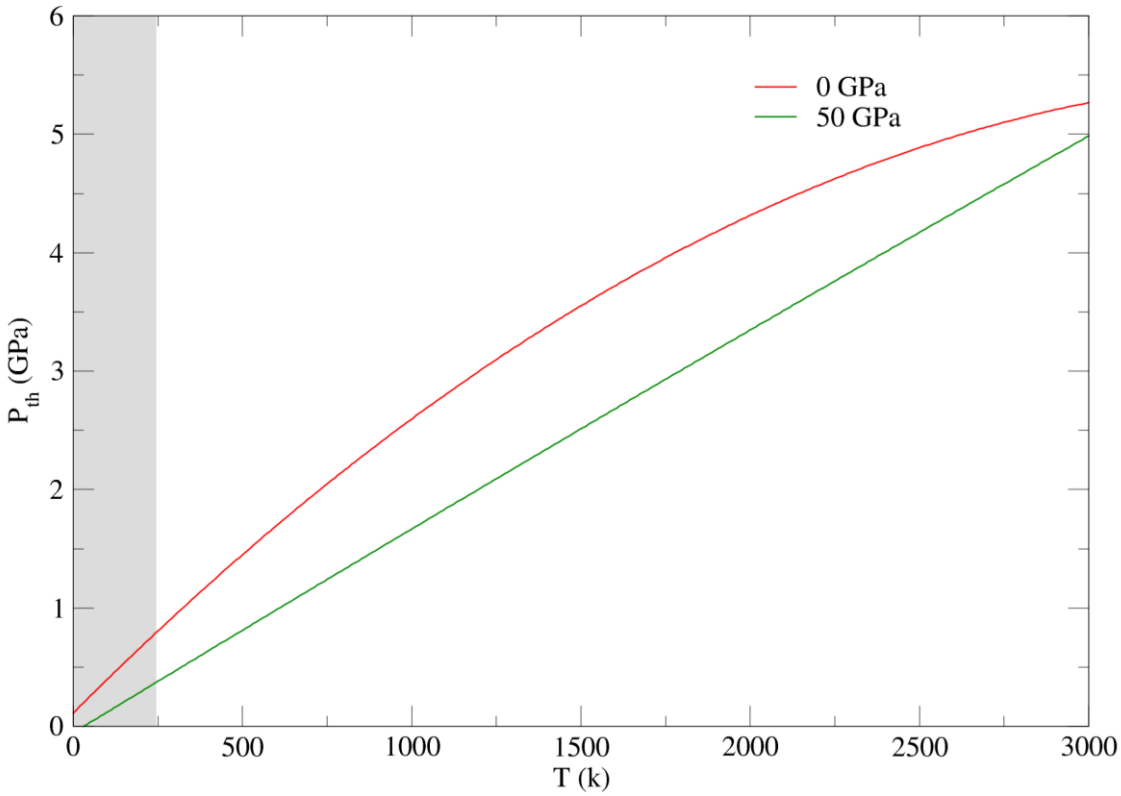

Figure 5.14: Temperature dependence of thermal pressure using QHA. Green line styles correspond to 50 GPa calculation and red line representation 0 GPa calculation.

We see that, for thermal pressure calculation, when we change the pressure from 0 GPa to 50 GPa, the linearity of thermal pressure with temperature increases as the pressure increases, which proves the fact that anharmonic effects is dominant at low pressure but suppressed at high pressure.

Root mean square displacement

Root mean square displacement measures the displacement of an atom from its equilibrium position at given interval of time. It `provides information about the nature of vibration of an atom. The variation of RMSD with temperature is evaluated using eq. 4.20 at pressure 0GPa and at pressure 50GPa using MD simulations (figure 5.15 and figure 5.16). We use the crystal whose volume is fixed at 300K and run NVT simulations to study the variation of RMSD at different temperature (figure 5.16).

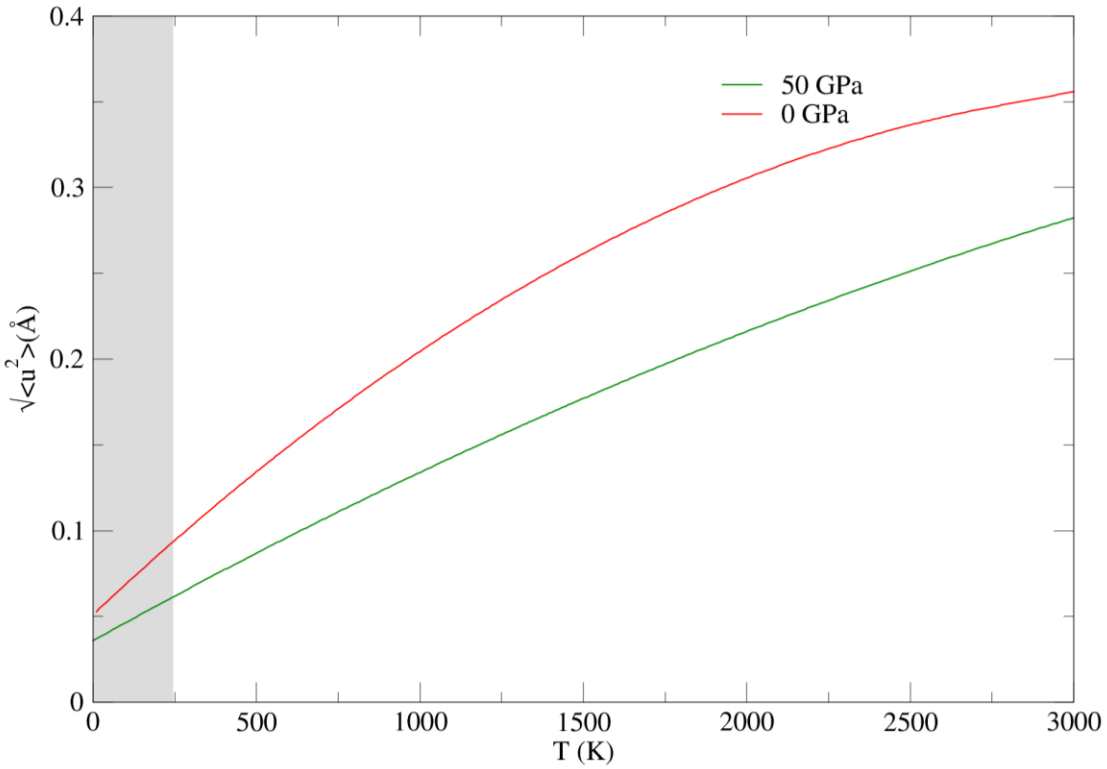

Figure 5.15: Temperature dependence of RMSD using MD calculation at pressure 0 GPa (red line) and 50GPa (green line).

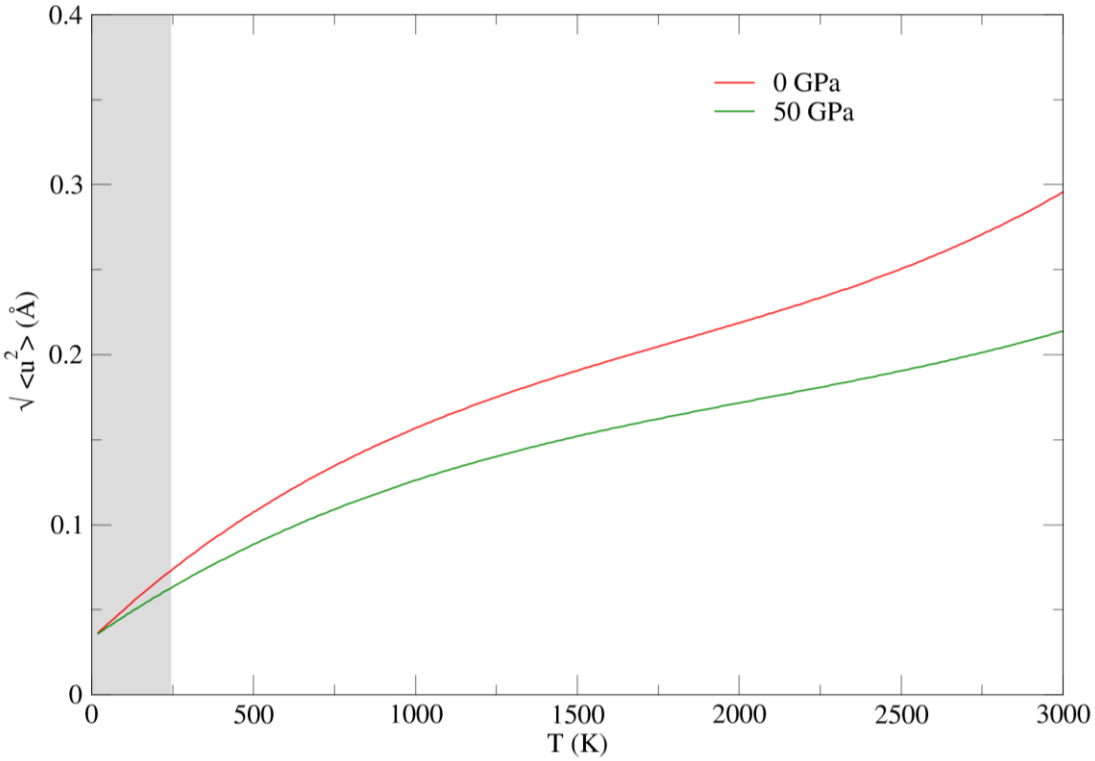

Figure 5.16: Temperature dependence of RMSD using MD calculation at pressure 0 GPa (red line) and 50GPa (green line) and volume fixed at 300K.

According to harmonic theory, the RMSD for harmonic system is constant but we are unable to see such behavior in tantalum even at very low temperature, which suggest that Ta is highly anharmonic in nature. The nonlinearity of RMSD at high temperature indicates the importance of the anharmonicity at high temperature regime. Since, high pressure in the system restricts the motion of particles thus lowering RMSD value for 50 GPa. RMSD also provides key information on nature of vibrational difference. We found that RMSD value goes down with increase in pressure due to the restriction in vibration of particles. The calculated value of RMSD lies within 10% of lattice constant which satisfies Lindemann criterion. RMSD can be related with entropy of the system which signifies the space available for particles in a system to fluctuate.

Chapter 6: Summary and Conclusion

To summarize, in certain conditions (especially at high temperature, properties like α, γ, especially at high temperatures) the role of intrinsic anharmonicity can be significantly important. So, in order to predict the accurate thermal EOS of solid, it is often necessary to account for intrinsic anharmonicity. The most common way to predict the degree of anharmonicity of system is the measure of Grüneisen parameter but we observe the anomaly in the difference between QHA and MD result. We assume that the huge difference between QHA results and MD in Grüneisen parameter is the due to the facts that phonons are temperature dependent rather than volume dependent due to which anharmonicity neglected by QHA, which becomes significant at high temperature. So, the unusual results in the low-temperature region can be corrected by measuring the entropy difference between MD and QHA calculation (intrinsic anharmonicity) using adiabatic switching method and by adding the anharmonic contribution in Grüneisen parameter. Plotting of anharmonicity shows the flattening of curve at high temperature, which suggest that that volume and temperature effects on the phonon energies are nearly equal and opposite at high temperature. Also, The Comparison of with atomic volume contribution to the entropy shows that temperature contribution plays significant role at low temperature but volume contribution at high temperature and this is the reason the difference is higher at low temperature. Since, taking account of higher order correction to anharmonicity and including temperature is still wrinkles in QHA and calculation of Grüneisen parameter employing DFT-QHA is impracticable. Thus, one can't rely on QHA in accurate prediction of thermal pressure and thus EOS of the system at high pressure.

References

[1] E. Grüneisen, Ann. Phys. **344**, 257 (1912).
[2] R. E. Cohen and O. Gülseren, Phys. Rev. B - Condens. Matter Mater. Phys. **63**, 1 (2001).
[3] S. Taioli, C. Cazorla, M. J. Gillan, and D. Alfè, Phys. Rev. B **75**, 214103 (2007).
[4] R. Ravelo and B. Holian, (2013). Unpublished.
[5] A. Dewaele, P. Loubeyre, and M. Mezouar, Phys. Rev. B **70**, 94112 (2004).
[6] L. Brillouin, Comptes Rendus Hebd. Des Séances L'Académie Des Sci. **191**, 292 (1930).
[7] H. J. Monkhorst and J. D. Pack, Phys. Rev. B **13**, 5188 (1976).
[8] C. Kittel, P. McEuen, and P. McEuen, *Introduction to Solid State Physics* (Wiley New York, 1976).
[9] P. W. Atkins and S. E. Novick, Am. J. Phys. **60**, 671 (1992).
[10] S. Deschanel, L. Vanel, N. Godin, E. Maire, G. Vigier, and S. Ciliberto, J. Phys. D. Appl. Phys. **42**, 214001 (2009).
[11] J. C. Slater, *Introduction to Chemical Physics* (Read Books Ltd, 2013).
[12] J. S. Dugdale and D. K. C. MacDonald, Phys. Rev. **89**, 832 (1953).
[13] V. N. Zubarev and V. Y. Vashchenko, Sov. Phys. Solid State **5**, 653 (1963).
[14] D. C. Wallace, *Thermodynamics of Crystals* (Courier Corporation, 1998).
[15] P. G. Grodzka, *Gruneisen Parameter Study* (LOCKHEED MISSILES AND SPACE CO INC HUNTSVILLE AL HUNTSVILLE ENGINEERING CENTER, 1967).
[16] R. Car and M. Parrinello, Phys. Rev. Lett. **55**, 2471 (1985).
[17] T. J. Barth, M. Griebel, D. E. Keyes, R. M. Nieminen, and D. Roose, (2007).
[18] J. A. Morrone and R. Car, Phys. Rev. Lett. **101**, 17801 (2008).
[19] L. Lin, J. A. Morrone, R. Car, and M. Parrinello, Phys. Rev. Lett. **105**, 110602 (2010).
[20] (n.d.).
[21] F. Kirchhoff, M. J. Mehl, N. I. Papanicolaou, D. A. Papaconstantopoulos, and F. S. Khan, Phys. Rev. B **63**, 195101 (2001).
[22] M. P. Allen and D. J. Tildesley, *Computer Simulation of Liquids* (Oxford university press, 2017).
[23] A. Rahman, Phys. Rev. **136**, A405 (1964).
[24] J. A. McCammon, B. R. Gelin, and M. Karplus, Nature **267**, 585 (1977).
[25] S. Nosé, Mol Phys **52: 255**, (1984).
[26] W. G. Hoover, Hoover WG Phys Rev A **34**, 2499 (1985).
[27] M. S. Daw and M. I. Baskes, Phys. Rev. Lett. **50**, 1285 (1983).
[28] M. S. Daw and M. I. Baskes, Phys. Rev. B **29**, 6443 (1984).
[29] M. S. Daw, S. M. Foiles, and M. I. Baskes, Mater. Sci. Reports **9**, 251 (1993).
[30] M. W. Finnis and J. E. Sinclair, Philos. Mag. A **50**, 45 (1984).
[31] F. Ercolessi, E. Tosatti, and M. Parrinello, Phys. Rev. Lett. **57**, 719 (1986).
[32] (n.d.).
[33] S. M. Foiles, Phys. Rev. B **48**, 4287 (1993).
[34] J. A. Moriarty, Phys. Rev. B **38**, 3199 (1988).
[35] R. Ravelo, T. C. Germann, O. Guerrero, Q. An, and B. L. Holian, Phys. Rev. B **88**, 134101 (2013).
[36] T. P. Straatsma, H. J. C. Berendsen, and J. P. M. Postma, J. Chem. Phys. **85**, 6720 (1986).
[37] M. Watanabe and W. P. Reinhardt, Phys. Rev. Lett. **65**, 3301 (1990).

[38] D. C. Wallace, *Entropy of Alkali Metals* (1992).
[39] J. M. Haile, Elem. Methods (1992).
[40] Y. S. Touloukian, R. K. Kirby, R. E. Taylor, and P. D. Desai, (1975).

Vitae

Bimal K C was born and raised in Nepal. He graduated from high school in 2006 at Prithvi Narayan Campus in Pokhara, Nepal. In 2007, he received a Merit Scholarship Award to pursue his Bachelor of Science at Tri-Chandra Campus (TC), Kathmandu, Nepal. He received his Bachelor of Science in 2011 from TC with a major in Physics. In 2011, he was selected to pursue his Master of Science at Amrit Campus (ASCOL), Kathmandu, Nepal. He received his Master of Science in 2016 from ASCOL with a major in Physics. In 2017, He was accepted to the Physics Master's program at The University of Texas at El Paso (UTEP), USA where he continued his education as an international student. In 2019 he received his Masters of Science in Physics. While student at UTEP, he worked as a teaching assistant.

Email: bkc@miners.utep.edu